Università degli Studi di Padova

Dipartimento di Fisica e Astronomia
"Galileo Galilei"

Corso di Laurea in Fisica

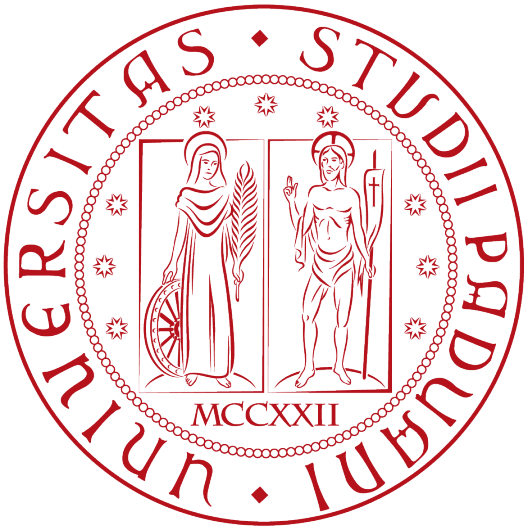

Tesi di Laurea

The Frozen-Flow Approximation and the formation of cosmic structures

Laureanda:
Amalia Basiricò

Relatore:
Prof. Sabino Matarrese

Anno Accademico 2017/2018

Contents

Introduction **ii**

1 Background evolution **1**
1.1 Geometrical structure of the Universe 1
1.2 Friedmann equations 1
1.2.1 Einstein-de Sitter model 2
1.3 Gravitational instability in the expanding Universe 3
1.3.1 Static background 4
1.3.2 Non-static background 4

2 Dynamics of a self-gravitating collisionless fluid **10**
2.1 The Zel'dovich approximation 13
2.2 The frozen-flow approximation 16

3 Understanding frozen-flow approximation **18**
3.1 Validity of the method 19
3.1.1 Toy model 20
3.1.2 Spherical top-hat model 21
3.2 Large-scale structure evolution 24

4 Beyond frozen-flow approximation **27**
4.1 Adhesion model 27
4.2 Viscid-flow approximation 31

Conclusion **34**

Introduction

Understanding the physical processes involved during the various phases of the gravitational collapse of matter is one of the most important issues in cosmology as the observed Universe owes these processes its large-scale structure. The early Universe was almost homogeneous exept slight perturbations in density that can be seen in the small degree of anisotropy of the cosmic microwave background radiation. These perturbations grow with time, by gravitational instability, giving rise to the distribution of matter we see today and to gravitationally bounded objects.

A complementary issue is that of trying to reconstruct the initial conditions of the clustering process starting from observational data such as the spatial distribution of galaxies or their peculiar velocities. In particular the clustering pattern of today's Universe gives information on the spectrum of the primordial perturbation and on the type of dark matter (if any), allowing the comprehension on how exactly the perturbations evolves with time. The reconstruction of the initial conditions is made by considering that, at the epoch of the large-scale structures formation, dark matter acts as collisionless dustlike particles without pressure and is governed by Newtonian gravitation only.

This problem can be dealt with in two different ways: the classical statistical approach, by calculating mean quantities and comparing them with theoretical predictions, and the dynamical approach, that aims to trace back the status of the present Universe starting from observational data to reconstruct the initial conditions.

The latter approach has gained attenction, as more and more data on peculiar velocity of galaxies, as well as very large and complete galaxy redshift surveys, have become available. It has been proved to be very useful in this kind of method, to extend theoretical predictions beyond the linear approximation for density, velocity and gravitational fields, making use of approximations valid in the mildly non-linear regime such as the celebrated Zel'dovich approximation.

Yet this method shows a main drawback, that is its inability to follow the developement of structures beyond the epoch of caustic formation, so in order to overcome this limitation many variants have been proposed besides this classical approach, among which the most promising one is the so called adhesion theory, where an artificial viscosity term is introduced in the Euler equation aiming to mimic the gravitational sticking of particles around pankakes.

Another approach to try to overcome the drawback caused by the impossibility of a description after shell-crossing is a new approximation scheme, called frozen-flow approximation, which allows an extrapolation beyond the time at which caustic would have occurred. This

is based on the idea of extrapolating the growing linear mode of the velocity field beyond its actual range of validity, while solving exactly the equation of continuity. Stream lines are then kept frozen to their initial shape, thus forcing the dynamics to remain in the laminar regime.

An advantage of this approximation is that the evolved density field is simply related to the peculiar velocity field, so it can be used as a fast easily implementable algorithm for reconstructing the actual density field in scales involved in moderately non-linear evolution.

In this work we will proceed as follows: in the first place we will articulate the properties of the evolution of the background and the formation of large-scale structures via gravitational instability in Chapter 1; in Chapter 2 we will give the general description of the dynamics of a self gravitating collinsionless fluid and then we will introduce the two approximation methods cited above: firsty the Zel'dovich one and then the frozen-flow.
We will give a more detailed description of the results provided by frozen-flow approximation in Chapter 3, compared to the one obtained through other descriptions.
Finally in Chapter 4 we will see how we can implement the frozen-flow method in order to get a more realistic description of the evolution of macroscopical structures, that is the so called viscid-flow approximation.

Chapter 1

Background evolution

1.1 Geometrical structure of the Universe

The first attempts to describe the properties of the Universe were made in the early years of the 18th century. Given the absence of solid empirical bases onto which building a model, some guide symmetry principles were introduced to reduce the number of degrees of freedom of the system.
In cosmology this has been done by the formulation of the cosmological principle [1]:

Every comoving observer sees the Universe around them, at a given time (in their reference frame), as homogeneous and isotropic.

where an operative definition of comoving is that a comoving observer will see the cosmic background radiation as isotropic, and the adjectives homogeneous and isotropic are referred to the mass-energy didtribution on a large-scale.

The geometrical properties of the Universe are expressed by its metric. The most general possible way to descibe the spacetime metric of a Universe in which the cosmological principle is valid, is the following:

$$ds^2 = c^2dt^2 - a^2(t)\left(\frac{dr^2}{1-kr^2} + r^2d\Omega^2\right) \tag{1.1}$$

called Robertson-Walker metric, where k is an adimensional parameter that describes the spatial curvature, scaled so as to take the value 0 to represent a flat space, or ± 1 in case of positive or negative curvature, whereas $a(t)$ is a function of the cosmological proper time, namely the time of a comoving observer, called *scale factor*.

1.2 Friedmann equations

In the previous section the Universe description given was substantially static, whereas its dynamic behaviour is determined by Friedmann's equations. These equations can be easily obtained from a Newtonian description of the gravitational field, however they should be

drawn from Einstein equations, imposing the symmetries of the system (i.e. the cosmological principle) and adding the cosmological constant Λ, achieving the following outcome:

$$\left(\frac{\dot{a}}{a}\right)^2 = \frac{8\pi G}{3}\rho + \frac{\Lambda c^2}{3} - \frac{kc^2}{a^2} \tag{1.2}$$

$$\frac{\ddot{a}}{a} = -\frac{4\pi G}{3}\left(\rho + 3\frac{P}{c^2}\right) + \frac{\Lambda c^2}{3} \tag{1.3}$$

$$\dot{\rho} = -3\frac{\dot{a}}{a}\left(\rho + \frac{P}{c^2}\right) \tag{1.4}$$

Only two of these equations are independent, therefore in order to find the explicit solutions for the quantities $a(t)$, $\rho(t)$ and $P(t)$ we need to make further assumptions by introducing an equation of state. We assume that our Universe is filled with a perfect fluid, characterized by isotropic energy density and pressure, so that

$$P = P(\rho)$$

this type of fluid is called *barotropic fluid*. We can suppose this relation to be linear

$$P = w\rho c^2,$$

where w is a dimensionless constat; substituting this expression in the third Friedmann equation (1.4) we get:

$$\dot{\rho} = -3(1+w)\frac{\dot{a}}{a}\rho \quad \Rightarrow \quad \frac{\dot{\rho}}{\rho} = -3(1+w)\frac{\dot{a}}{a} \quad \Rightarrow \quad \rho \propto a^{-3(1+w)} \tag{1.5}$$

then substituting the result in the first Friedmann equation (1.2) we can solve for a, but that's not analitically possible. In order to obtain some solutions we have to consider particular cases according to the value taken by w. We will analyze only the case in which w is equal to zero that describes a Universe dominated by matter (both ordinary and dark) made of non-relativistic particles (it's the case of CDM). In this description it turns out to be $P = 0$, that is pressure is either null or anyhow neglectible with respect to the energy density. Therefore $\rho \propto a^{-3}$ and so mass (number of particles) is conserved.

1.2.1 Einstein-de Sitter model

We want to solve Friedmann equations, considering the equation of state $P = w\rho c^2$, in order to find explicit expressions for $a(t)$, $\rho(t)$ and $P(t)$. The rearranged third equation (1.5) gave:

$$\rho(t) = \rho_* \left(\frac{a(t)}{a_*}\right)^{-3(1+w)}$$

The first Friedmann equation shows that for $w > -\frac{1}{3}$, the first term dominates over the others, so neglecting them and substituting ρ:

$$\dot{a}^2 = \underbrace{\frac{8\pi G}{3}\rho_* a_*^{3(1+w)}}_{\equiv A^2} a^{2-3(1+w)} = A^2 a^{2-3(1+w)} \qquad \Rightarrow \qquad \dot{a} = \pm A a^{-\frac{1+3w}{2}}$$

$$\Rightarrow \quad a^{\frac{1+3w}{2}} \mathrm{d}a = \pm A \mathrm{d}t$$

choosing the positive solution, for the experimantal observations tell us that the Universe is expanding, and integrating, one gets:

$$a(t) = a_* \left[1 + \frac{3}{2}(1+w)H_*(t-t_*)\right]^{\frac{2}{3(1+w)}} \qquad H_* = \sqrt{\frac{8\pi G}{3}\rho_*}$$

by substituting this result in the expressions for ρ and H, one gets:

$$\rho(t) = \rho_* \left[1 + \frac{3}{2}(1+w)H_*(t-t_*)\right]^{-2} \qquad H(t) = H_* \left[1 + \frac{3}{2}(1+w)H_*(t-t_*)\right]^{-1}.$$

Though the Friedmann equations are formally solved at this point, it is useful to re-express the results using a new temporal variable:

$$t = t' - t_{\mathrm{BB}} = t' - t_* + \frac{2}{3}\frac{H_*^{-1}}{1+w},$$

where t_{BB} is the time at which the part of the scale factor expression in brackets, is equal to zero, and t' takes the place of the former t. In this way we have:

$$a(t) \propto t^{\frac{2}{3(1+w)}} \qquad \rho(t) = \frac{1}{6(1+w)^2\pi G}t^{-2} \qquad H(t) = \frac{2}{3(1+w)}\,t^{-1}.$$

In case of a non-relativistic matter dominated Universe ($w = 0$), we obtain:

$$a(t) \propto t^{\frac{2}{3}} \qquad \rho(t) = \frac{1}{6\pi G}t^{-2} \qquad H(t) = \frac{2}{3}\,t^{-1}.$$

1.3 Gravitational instability in the expanding Universe

After having analysed the equations that rule the Universe dynamics, we want to explain how the formation of large-scale structures has been possible, starting from an almost uniform pattern. The key idea in explaining the way in which structures evolve in the universe is gravitational instability, a model whose father is Sir James Jeans.
According to Jeans' theory in a homogeneous and isotropic fluid, small fluctuations in density $\delta\rho$, or in velocity δv, lead to gravitationally bounded objects as they could evolve with time; therefore now our purpose will be studying the gravitational instability of a fluid.

The presupposition from which we start are the fluid equations:

Euler equation	$\frac{\mathrm{D}\mathbf{v}}{\mathrm{D}t} = -\frac{1}{\rho}\nabla p - \nabla\Phi$
Continuity equation	$\frac{\mathrm{D}\rho}{\mathrm{D}t} + \rho\nabla\cdot\mathbf{v} = 0$
Poisson equation	$\nabla^2\Phi = 4\pi G\rho$

1.3.1 Static background

By following Jeans' argument we will assume that the Universe is static instead of in expansion, as it was believed to be during those years. This assumption will lead to poorly evaluate the velocity of the gravitational collapse, in detail it will extimate its growth to be exponential.
The main problem that induced Jeans to consider the case of a static background was that there's no analitical solution for the fluid equations in the general case. A perturbative approach has to be used, for we can't solve them: we choose simple background solutions and then add to them some perturbations. Jeans used a set of background solutions that he knew weren't consistent:

$$\rho = \text{cost.} \qquad v = 0 \qquad P = \text{cost.} \qquad \Phi = \text{cost} \qquad s = \text{cost.}$$

The inconsistency of these solutions comes from Poisson equation, for we can't have simultaneously $\rho = \text{cost.} \neq 0$ and $\Phi = \text{cost.}$ As we're not interested in a static description of the Universe we will drop this argument, therefore we will focus on a non-static background solution.

1.3.2 Non-static background

In order to find a non-static background solution we use the coordinates $\mathbf{r} = a\mathbf{x}$ which have the property of being inertial with respect to the Friedmann-Robertson-Walker background evolution. One has:

$$\mathbf{w} = \dot{\mathbf{r}} = \frac{\dot{a}}{a}\mathbf{r} + a\frac{\mathrm{d}\mathbf{x}}{\mathrm{d}t} \equiv H\mathbf{r} + \mathbf{v} = \mathbf{v}_b + \mathbf{v}$$

where $\mathbf{v}_b$ is the background velocity and $\mathbf{v}$ is called *peculiar velocity*. The gradient with respect to r is binded to the gradient with respect to x by the following relation:

$$\nabla_{\mathbf{r}} \equiv \frac{\partial}{\partial\mathbf{r}} = \frac{1}{a}\frac{\partial}{\partial\mathbf{x}} = \frac{1}{a}\nabla_{\mathbf{x}}.$$

For a generic function $f(\mathbf{r}, t)$ one has

$$\begin{aligned}\frac{\mathrm{D}f(\mathbf{r},t)}{\mathrm{D}t} &= \left.\frac{\partial f}{\partial t}\right|_{\mathbf{r}} + \frac{\partial f}{\partial\mathbf{r}}\dot{\mathbf{r}} \\ &= \left.\frac{\partial f}{\partial t}\right|_{\mathbf{r}} + H(\mathbf{r}\cdot\nabla_{\mathbf{r}})f + (\mathbf{v}\cdot\nabla_{\mathbf{r}})f.\end{aligned}$$

and rewriting the same f as a function of $\mathbf{x}$ and t, we find

$$\frac{\mathrm{D}f(\mathbf{x},t)}{\mathrm{D}t} = \left.\frac{\partial f}{\partial t}\right|_{\mathbf{x}} + \frac{\partial f}{\partial \mathbf{x}}\dot{\mathbf{x}} = \left.\frac{\partial f}{\partial t}\right|_{\mathbf{x}} + \frac{1}{a}(\mathbf{v}\cdot\nabla_{\mathbf{x}})f.$$

But, as the two convective derivatives have to be equal, we have

$$\left.\frac{\partial f}{\partial t}\right|_{\mathbf{x}} = \left.\frac{\partial f}{\partial t}\right|_{\mathbf{r}} + H(\mathbf{r}\cdot\nabla_{\mathbf{x}})f.$$

Using the coordinates $\mathbf{r}$ the fluid equations take the standard Newtonian form, so assuming constant entropy (i.e. we are considering adiabatic perturbations) we can write

$$\left.\frac{\partial \rho}{\partial t}\right|_{\mathbf{r}} + \nabla_{\mathbf{r}}(\rho\mathbf{w}) = 0 \tag{1.6a}$$

$$\left.\frac{\partial \mathbf{w}}{\partial t}\right|_{\mathbf{r}} + (\mathbf{w}\cdot\nabla_{\mathbf{r}})\mathbf{w} = -\frac{1}{\rho}\nabla_{\mathbf{r}}p - \nabla_{\mathbf{r}}\Phi \tag{1.6b}$$

$$\nabla^2_{\mathbf{r}}\Phi = 4\pi G\rho \tag{1.6c}$$

We want to study the behavour of the system when it undergoes a linear perturbation, so we are searching for linear perturbative solutions to these equations; therefore we introduce the perturbation of the density field in the homogeneous background $\delta\rho$, and the *peculiar gravitational potential* ϕ which expresses the fluctuations of gravitational potential:

$$\rho = \rho_b + \delta\rho \qquad\qquad \Phi = \Phi_b + \phi\ ,$$

so that instead of (1.6c) we obtain

$$\nabla^2_{\mathbf{r}}\Phi_b = 4\pi G\rho_b(t) \qquad \Rightarrow \qquad \Phi_b = \frac{2\pi G}{3}\rho_b(t)r^2$$

$$\nabla^2_{\mathbf{r}}\phi = 4\pi G\delta\rho \qquad \Rightarrow \qquad \nabla^2_{\mathbf{x}}\phi = 4\pi G a^2\delta\rho \tag{1.7}$$

where (1.7) is the *cosmological Poisson equation*. It is worth noting that the density source $\delta\rho$ can be whether positive or negative. Now we want to express our quantities according to the comoving coordinate $\mathbf{x}$ and to eliminate all background terms from the equations.
The continuity equation (1.6a) gives

$$\left.\frac{\partial \rho}{\partial t}\right|_{\mathbf{x}} - H(\mathbf{r}\cdot\nabla_{\mathbf{r}})\rho + \rho\nabla_{\mathbf{r}}(H\mathbf{r}+\mathbf{v}) + H(\mathbf{r}\cdot\nabla_{\mathbf{r}})\rho + (\mathbf{v}\cdot\nabla_{\mathbf{r}})\rho = 0$$

$$\left.\frac{\partial \rho}{\partial t}\right|_{\mathbf{x}} + \rho\nabla_{\mathbf{r}}(H\mathbf{r}+\mathbf{v}) + (\mathbf{v}\cdot\nabla_{\mathbf{r}})\rho = 0$$

$$\left.\frac{\partial \rho}{\partial t}\right|_{\mathbf{x}} + 3H\rho + \rho\left(\nabla_{\mathbf{r}}\mathbf{v}\right) + \left(\mathbf{v}\cdot\nabla_{\mathbf{r}}\right)\rho = 0$$

$$\Rightarrow \qquad \left.\frac{\partial \rho}{\partial t}\right|_{\mathbf{x}} + 3H\rho + \frac{1}{a}\nabla_{\mathbf{x}}(\rho\mathbf{v}) = 0 \tag{1.8}$$

The Euler equation (1.6b) gives

$$\left.\frac{\partial \mathbf{v}}{\partial t}\right|_{\mathbf{r}} + \underline{\left.\frac{\partial (H\mathbf{r})}{\partial t}\right|_{\mathbf{r}}} + \underline{(H\mathbf{r}\cdot\nabla_{\mathbf{r}})(H\mathbf{r})} + (\mathbf{v}\cdot\nabla_{\mathbf{r}})(H\mathbf{r}) + (H\mathbf{r}\cdot\nabla_{\mathbf{r}})\mathbf{v} + (\mathbf{v}\cdot\nabla_{\mathbf{r}})\mathbf{v} = -\frac{1}{\rho}\nabla_{\mathbf{r}} p - \underline{\nabla_{\mathbf{r}}\Phi_b} - \nabla_{\mathbf{r}}\phi$$

the underlined terms refer to the background and their sum has to equate to zero:

$$\left.\frac{\partial (H\mathbf{r})}{\partial t}\right|_{\mathbf{r}} + (H\mathbf{r}\cdot\nabla_{\mathbf{r}})(H\mathbf{r}) = -\nabla_{\mathbf{r}}\Phi_b$$

$$\left.\frac{\partial (H\mathbf{r})}{\partial t}\right|_{\mathbf{x}} - (H\mathbf{r}\cdot\nabla_{\mathbf{r}})(H\mathbf{r}) + (H\mathbf{r}\cdot\nabla_{\mathbf{r}})(H\mathbf{r}) = -\frac{4\pi G}{3}\rho_b\mathbf{r}$$

$$\dot{H}\mathbf{r} + H\left.\frac{\partial \mathbf{r}}{\partial t}\right|_{\mathbf{x}} = -\frac{4\pi G}{3}\rho_b\mathbf{r}\,.$$

As we are referring to the background the only non-zero component of $\left.\frac{\partial \mathbf{r}}{\partial t}\right|_{\mathbf{x}}$ is $\mathbf{v}_b = H\mathbf{r}$, so the expression becomes

$$(\dot{H} + H^2)\mathbf{r} = -\frac{4\pi G}{3}\rho_b\mathbf{r}\,.$$

This is proven to be satisfied by combining the results for (1.8) and for the first Friedmann equation applied on background:

$$\begin{cases} \dot{\rho} = -3H\rho \\ H^2 = \frac{8\pi G}{3}\rho \end{cases} \qquad \Rightarrow \qquad \dot{H} = -4\pi G\rho\,,$$

therefore substituting $\dot{H}$ and H^2 in the former equation this becomes an identity. Thus the Euler equation can be written as follows

$$\left.\frac{\partial \mathbf{v}}{\partial t}\right|_{\mathbf{r}} + H\mathbf{v} + (H\mathbf{r}\cdot\nabla_{\mathbf{r}})\mathbf{v} + (\mathbf{v}\cdot\nabla_{\mathbf{r}})\mathbf{v} = -\frac{1}{\rho}\nabla_{\mathbf{r}} p - \nabla_{\mathbf{r}}\phi$$

and by expressing each term according to the comoving coordinates, one finally gets

$$\frac{\partial \mathbf{v}}{\partial t} + H\mathbf{v} + \frac{1}{a}(\mathbf{v}\cdot\nabla_{\mathbf{x}})\mathbf{v} = -\frac{1}{a\rho}\nabla_{\mathbf{x}} p - \frac{1}{a}\nabla_{\mathbf{x}}\phi \tag{1.9}$$

Now the obtained equations (1.7), (1.8) and (1.9) can be linearized; writing $\delta\rho = \rho_b\delta$ and substituting $\rho = \rho_b + \delta\rho \equiv \rho_b(1+\delta)$ in the continuity equation (1.8):

$$(1+\delta)\Big(\frac{\partial \rho_b}{\partial t} + 3H\rho_b\Big) + \rho_b\frac{\partial \delta}{\partial t} + \frac{1}{a}\nabla_{\mathbf{x}}\cdot(\rho\mathbf{v}) = 0$$

the term $\frac{\partial \rho_b}{\partial t} + 3H\rho_b$ is equal to zero, since $\dot{\rho}_b = -3H\rho_b$ as we have seen. Therefore by neglecting all the non-linear perturbational terms one gets

$$\rho_b\dot{\delta} + \frac{1}{a}\rho_b\nabla_{\mathbf{x}}\cdot\mathbf{v} = 0 \qquad \Rightarrow \qquad \dot{\delta} + \frac{1}{a}\nabla_{\mathbf{x}}\cdot\mathbf{v} = 0 \tag{1.10}$$

As concerns Euler equation, its linearized version can be easily found by simply neglicting the term $(\mathbf{v}\cdot\nabla_{\mathbf{x}})\mathbf{v}$, for $\mathbf{v}$ is already a perturbation:

$$\frac{\partial \mathbf{v}}{\partial t} + H\mathbf{v} = -\frac{1}{a\rho}\nabla_{\mathbf{x}} p - \frac{1}{a}\nabla_{\mathbf{x}}\phi. \tag{1.11}$$

No further manipulation needs to be done to the cosmological Poisson equation since it is already linear.
Moving to Fourier space the perturbations are expanded as follows

$$\delta(\mathbf{x},t) = \frac{1}{(2\pi)^3}\int \mathrm{d}^3k\, e^{i\mathbf{k}\cdot\mathbf{x}}\,\delta_{\mathbf{k}}(t)$$
$$\mathbf{v}(\mathbf{x},t) = \frac{1}{(2\pi)^3}\int \mathrm{d}^3k\, e^{i\mathbf{k}\cdot\mathbf{x}}\,\mathbf{v}_{\mathbf{k}}(t)$$
$$\phi(\mathbf{x},t) = \frac{1}{(2\pi)^3}\int \mathrm{d}^3k\, e^{i\mathbf{k}\cdot\mathbf{x}}\,\phi_{\mathbf{k}}(t)$$

hence substituting these expressions in the linearized equations (1.10), (1.11) and (1.9), one obtains a linearization for each mode $\mathbf{k}$. Then, (1.10) becomes

$$\frac{1}{(2\pi)^3}\int \mathrm{d}^3k\Big[e^{i\mathbf{k}\cdot\mathbf{x}}\,\dot\delta(\mathbf{k},t) + \frac{1}{a}\big(\nabla_{\mathbf{x}}\, e^{i\mathbf{k}\cdot\mathbf{x}}\big)\mathbf{v}(\mathbf{k},t)\Big] = 0$$

$$\frac{1}{(2\pi)^3}\int \mathrm{d}^3k\, e^{i\mathbf{k}\cdot\mathbf{x}}\left[\dot\delta(\mathbf{k},t) + \frac{i}{a}\mathbf{k}\cdot\mathbf{v}(\mathbf{k},t)\right] = 0$$

$$\Rightarrow \quad \dot\delta_{\mathbf{k}} + i\frac{\mathbf{k}\cdot\mathbf{v}_{\mathbf{k}}}{a} = 0 \tag{1.12}$$

whereas (1.11) gives

$$\frac{1}{(2\pi)^3}\int \mathrm{d}^3k\, e^{i\mathbf{k}\cdot\mathbf{x}}\left[\dot{\mathbf{v}}(\mathbf{k},t) + H\mathbf{v}(\mathbf{k},t)\right] = -\frac{1}{a\rho_b}\nabla_{\mathbf{x}}\frac{\partial\rho}{\partial p}\,p + \frac{1}{a}\nabla_{\mathbf{x}}\phi$$

$$\frac{1}{(2\pi)^3}\int \mathrm{d}^3k\, e^{i\mathbf{k}\cdot\mathbf{x}}\left[\dot{\mathbf{v}}(\mathbf{k},t) + H\mathbf{v}(\mathbf{k},t)\right] = -\frac{\rho_b}{a\rho_b}\Big(\frac{\partial p}{\partial\rho}\Big)\nabla_{\mathbf{x}}\delta + \frac{1}{a}\nabla_{\mathbf{x}}\phi$$

$$\frac{1}{(2\pi)^3}\int \mathrm{d}^3k\, e^{i\mathbf{k}\cdot\mathbf{x}}\left[\dot{\mathbf{v}}(\mathbf{k},t) + H\mathbf{v}(\mathbf{k},t)\right] = -\frac{1}{a}\frac{1}{(2\pi)^3}\int \mathrm{d}^3k\big(\nabla_{\mathbf{x}}\, e^{i\mathbf{k}\cdot\mathbf{x}}\big)\Big[\Big(\frac{\partial p}{\partial\rho}\Big)\delta(\mathbf{k},t) + \phi(\mathbf{k},t)\Big]$$

$$\frac{1}{(2\pi)^3}\int \mathrm{d}^3k\, e^{i\mathbf{k}\cdot\mathbf{x}}\left[\dot{\mathbf{v}}(\mathbf{k},t) + H\mathbf{v}(\mathbf{k},t)\right] = -\frac{1}{a}\frac{1}{(2\pi)^3}\int \mathrm{d}^3k\; i\mathbf{k}\, e^{i\mathbf{k}\cdot\mathbf{x}}\left[\Big(\frac{\partial p}{\partial\rho}\Big)\delta(\mathbf{k},t) + \phi(\mathbf{k},t)\right]$$

$$\Rightarrow \quad \dot{\mathbf{v}}_{\mathbf{k}} + H\mathbf{v}_{\mathbf{k}} = -\frac{i\mathbf{k}}{a}\big(c_s^2\delta_{\mathbf{k}} + \phi_{\mathbf{k}}\big) \qquad c_s^2 \equiv \frac{\partial p}{\partial\rho} \tag{1.13}$$

Finally, cosmological Poisson equation can be expressed as

$$\frac{1}{(2\pi)^3}\int \mathrm{d}^3k\,\Big(\nabla_{\mathbf{x}}^2\, e^{i\mathbf{k}\cdot\mathbf{x}}\Big)\phi(\mathbf{k},t) = -\frac{4\pi G\rho_b a^2}{(2\pi)^3}\int \mathrm{d}^3k\, e^{i\mathbf{k}\cdot\mathbf{x}}\delta(\mathbf{k},t)$$

$$\frac{1}{(2\pi)^3}\int \mathrm{d}^3k\big(-k^2\big)e^{i\mathbf{k}\cdot\mathbf{x}}\,\phi(\mathbf{k},t) = -\frac{4\pi G\rho_b a^2}{(2\pi)^3}\int \mathrm{d}^3k\, e^{i\mathbf{k}\cdot\mathbf{x}}\delta(\mathbf{k},t)$$

$$\Rightarrow \quad k^2\phi_{\mathbf{k}} = -4\pi G a^2\rho_b(t)\delta_{\mathbf{k}} \tag{1.14}$$

In order to proceed with the description we will now use the *Kelvin circulation theorem*:

In an inviscid, barotropic flow with conservative body forces, the circulation around a closed curve moving with the fluid remains constant with time.

$$\frac{\mathrm{D}\Gamma}{\mathrm{D}t} = 0\,,$$

recalling that the circuitation Γ is defined as

$$\Gamma = \oint_\gamma \boldsymbol{\omega}\cdot\mathrm{d}\mathbf{l}\,,$$

where $\boldsymbol{\omega} = \nabla\times\mathbf{w}$ is the *vorticity* (in our case $\mathbf{w}$ takes the place of the general $\mathbf{v}$), so:

$$\frac{\mathrm{d}}{\mathrm{d}t}\oint_\gamma \boldsymbol{\omega}\cdot\mathrm{d}\mathbf{l} = \frac{\mathrm{d}}{\mathrm{d}t}\oint_\gamma \nabla\times\mathbf{w}\cdot\mathrm{d}\mathbf{l} = \oint_\gamma \frac{\mathrm{d}}{\mathrm{d}t}(\nabla\times\mathbf{w})\cdot\mathrm{d}\mathbf{l} = 0$$

$$\Rightarrow \quad \frac{\mathrm{d}}{\mathrm{d}t}\left[\nabla\times(H\mathbf{r}+\mathbf{v})\right] = \nabla\times\left(\dot{H}\mathbf{r} + H\frac{\mathrm{d}}{\mathrm{d}t}\mathbf{r} + \frac{\mathrm{d}}{\mathrm{d}t}\mathbf{v}\right) =$$
$$= \nabla\times\left(\dot{H}\mathbf{r} + H^2\mathbf{r} + H\mathbf{v} + \frac{\mathrm{d}}{\mathrm{d}t}\mathbf{v}\right) = 0 \quad \Rightarrow \quad \nabla\times(H\mathbf{v}+\dot{\mathbf{v}}) = 0\,,$$

therefore, since the quantity $\dot{\mathbf{v}} + H\mathbf{v}$ is proved to be irrotational, it can be described by the gradient of a scalar field. If we go to the Fourier space we find that $\dot{\mathbf{v}}_{\mathbf{k}} + H\mathbf{v}_{\mathbf{k}}$ is parallel to $\mathbf{k}$; as a consequence the orthogonal component in relation to $\mathbf{k}$, $\mathbf{v}_\perp$, obeys the equation:

$$\dot{\mathbf{v}}_\perp + H\mathbf{v}_\perp = 0 \qquad \Rightarrow \qquad \mathbf{v}_\perp \propto \frac{1}{a}\,.$$

Therefore we are allowed to consider only the component parallel to $\mathbf{k}$ relative to the peculiar velocity in the previuos equations (1.12) and (1.13).

By differentiation (1.12) reads:

$$\ddot{\delta}_{\mathbf{k}} + \frac{ik}{a}\dot{\mathbf{v}}_{\mathbf{k}} - \frac{ik}{a}H\mathbf{v}_{\mathbf{k}} = 0 \tag{1.15}$$

replacing equation (1.13) in (1.15) we obtain

$$\ddot{\delta}_{\mathbf{k}} + \frac{ik}{a}\Big[-Hv_{\mathbf{k}} - \frac{ik}{a}\big(c_s^2\delta_{\mathbf{k}} + \phi_{\mathbf{k}}\big)\Big] - \frac{ik}{a}Hv_{\mathbf{k}} = 0$$

then using (1.14) and (1.12)

$$\ddot{\delta}_{\mathbf{k}} + 2H\dot{\delta}_{\mathbf{k}} + \Big(\frac{c_s^2k^2}{a^2} - 4\pi G\rho_b\Big)\delta_{\mathbf{k}} = 0.$$

We can define a comoving Jeans wavenumber:

$$k_J = a\frac{\sqrt{4\pi G\rho_b}}{c_s}$$

for $k \ll k_J$ one can approximate the former equation as:

$$\ddot{\delta}_{\mathbf{k}} + 2H\dot{\delta}_{\mathbf{k}} - 4\pi G\rho_b\delta_{\mathbf{k}} \approx 0.$$

In the Einstein-de Sitter model we have

$$a \propto t^{\frac{2}{3}}, \qquad H = \frac{2}{3t}, \qquad \rho_b = (6\pi G t^2)^{-1}$$

so we obtain:

$$\ddot{\delta}_{\mathbf{k}} + \frac{4}{3t}\dot{\delta}_{\mathbf{k}} - \frac{2}{3t^2}\delta_{\mathbf{k}} \approx 0.$$

We can look for a solution of the form $\delta \propto t^\alpha$, hence for α:

$$3\alpha^2 + \alpha - 2 = 0 \qquad \Rightarrow \qquad \alpha = \frac{2}{3},\ \alpha = -1$$

in the two cases we have:

$$\delta_{\mathbf{k}} \propto \begin{cases} t^{\frac{2}{3}} & \rightarrow \quad \textit{growing mode} \\ t^{-1} & \rightarrow \quad \textit{decaying mode} \end{cases}$$

Replacing $\delta_{\mathbf{k}}$ in (1.13) and (1.14)

$$v_{\mathbf{k}} \propto \begin{cases} t^{\frac{1}{3}} \\ t^{-\frac{4}{3}} \end{cases} \qquad\qquad \phi_{\mathbf{k}} \propto \begin{cases} \text{const} \\ t^{-\frac{5}{3}} \end{cases}$$

Therefore those that were exponential solutions in the static background model, now are replaced by these solutions which grow as a power of time. This happens because the expansion of the Universe interferes with the gravitational collapse.
For each quantity we have a solution that is the sum of the two modes; for example, the time evolution of density, given the initial condition, gives:

$$\delta(t) = \delta_+(t_0)\left(\frac{t}{t_0}\right)^{\frac{2}{3}} + \delta_-(t_0)\left(\frac{t}{t_0}\right)^{-1},$$

where $\delta_\pm(t_0)$ represent the amplitudes of the growing $(+)$ and the decaying $(-)$ mode at the initial moment.
Summarizing, the growing-mode solution has the form:

$$\delta \propto t^{\frac{2}{3}} \propto a$$

$$v \propto t^{\frac{1}{3}}$$

$$\phi = \text{const.}$$

Chapter 2

Dynamics of a self-gravitating collisionless fluid

The description of a system composed by an ensemble of particles can be provided using two different, but equivalent approaches: the Lagrangian or the Eulerian one.
We will start our discussion considering a Lagrangian description, which, assuming the validity of Friedmann equations for the dynamics of a particle, leads to the *Euler-Lagrange equation*:

$$\frac{\mathrm{d}\mathbf{v}}{\mathrm{d}t} + H\mathbf{v} = -\frac{1}{a}\nabla\phi\,.$$

This equation has the same form of the Euler fluid equation provided the convective derivative is used in the latter. We are allowed to neglect the term connected to the pressure, for we are considering a very large range of scale for Cold Dark Matter[2].
Using comoving coordinates the Euler equation yields:

$$\frac{\mathrm{D}\mathbf{v}}{\mathrm{D}t} + 2\frac{\dot{a}}{a}\mathbf{v} = -\frac{1}{a^2}\nabla\phi \tag{2.1}$$

where $\mathbf{v}$ now is the *comoving* peculiar velocity $\mathbf{v}(\mathbf{x},t) \equiv \dot{\mathbf{x}}$. The equivalence between the two forms of the Euler equation can be shown with a few algebric passages:

$$\frac{\mathrm{D}\mathbf{v}}{\mathrm{D}t} + 2\frac{\dot{a}}{a}\mathbf{v} = -\frac{1}{a^2}\nabla\phi$$

$$a\frac{\mathrm{D}\mathbf{v}}{\mathrm{D}t} + \dot{a}\mathbf{v} + \dot{a}\mathbf{v} = -\frac{1}{a}\nabla\phi$$

$$\frac{\mathrm{D}a\mathbf{v}}{\mathrm{D}t} + \dot{a}\mathbf{v} = -\frac{1}{a}\nabla\phi$$

$$\frac{\mathrm{D}\mathbf{v}'}{\mathrm{D}t} + \frac{\dot{a}}{a}\mathbf{v}' = -\frac{1}{a}\nabla\phi$$

where we have called $\mathbf{v}'$ the non-comoving peculiar velocity defined at the beginning of the

chapter as $\mathbf{v} = a\dot{\mathbf{x}}$ to avoid redundances in notation. We shall assume that the Universe is spacially flat (Einstein-de Sitter) and matter dominated, so that the scale factor reads $a(t) = a_0 \left(\frac{t}{t_0}\right)^{\frac{2}{3}}$.
The continuity equation for the matter density becomes

$$\frac{\partial \rho}{\partial t} + 3H\rho + \frac{1}{a}\nabla(\rho \mathbf{v}') = 0$$

$$\frac{\partial \rho}{\partial t} + 3H\rho + \rho\nabla\cdot\mathbf{v} + (\mathbf{v}\cdot\nabla)\rho = 0$$

$$\Rightarrow \quad \frac{\mathrm{D}\rho}{\mathrm{D}t} + 3H\rho + \rho\nabla\cdot\mathbf{v} = 0 \tag{2.2}$$

while the peculiar gravitational potential is determined by local density inhomogeneities $\delta \equiv \frac{\rho(\mathbf{x},t)-\overline{\rho}(t)}{\overline{\rho}(t)}$, with $\overline{\rho}(t) = \overline{\rho}_0 \frac{a_0^3}{a^3}$ the mean mass density, through the Poisson equation, recalling that the Friedmann equations gave $H^2 = \frac{8\pi G}{3}\overline{\rho}$ and $\delta\rho = \rho - \overline{\rho}$

$$\nabla^2\phi = 4\pi G a^2 \delta\rho$$

$$\nabla^2\phi = 4\pi G a^2(\rho - \overline{\rho})\frac{\overline{\rho}}{\overline{\rho}}$$

$$\Rightarrow \quad \nabla^2\phi = \frac{3}{2}\dot{a}^2\delta \tag{2.3}$$

It will prove convenient to use rescaled variables for the velocity field, the density field and the local gravitational potential

$$\mathbf{u} \equiv \frac{\mathrm{d}\mathbf{x}}{\mathrm{d}a} = \frac{\mathbf{v}}{\dot{a}} \qquad \eta \equiv \frac{\rho a^3}{\overline{\rho}_0 a_0^3} \qquad \varphi \equiv \left(\frac{3t_0^2}{2a_0^3}\right)\phi\,,$$

according to these definitions $\delta = \eta - 1$. The equations (2.1), (2.2) and (2.3) can be rewritten as follows: starting with the the Euler equation (2.1), we have

$$a\dot{a}\frac{\partial \mathbf{u}}{\partial a} + a\ddot{a}\mathbf{u} + a(\dot{a}\mathbf{u}\cdot\nabla)(\dot{a}\mathbf{u}) + 2\dot{a}^2\mathbf{u} = -\frac{1}{a^2}\frac{2a_0^3}{3t_0^2}\nabla\varphi$$

deriving $a(t) = a_0 \left(\frac{t}{t_0}\right)^{\frac{2}{3}}$ with respect to time one gets

$$\dot{a} = \frac{2}{3}\frac{a}{t} \qquad \ddot{a} = -\frac{2}{9}\frac{a}{t^2}$$

and replacing them in the equation we obtain:

$$\frac{\mathrm{D}\mathbf{u}}{\mathrm{D}a} + \frac{3}{2a}\mathbf{u} = -\frac{3}{2a}\nabla\varphi \tag{2.4}$$

Rearranging the continuity equation (2.2), we have

$$\frac{\partial}{\partial t}\left(\frac{\rho_0^3 a_0^3 \eta}{a^3}\right) + 3\frac{\dot{a}}{a}\frac{\rho_0^3 a_0^3 \eta}{a^3} + \frac{\rho_0^3 a_0^3 \eta}{a^3}\nabla\dot{a}\mathbf{u} + \dot{a}\mathbf{u}\nabla\frac{\rho_0^3 a_0^3 \eta}{a^3} = 0$$

$$\frac{1}{a^3}\frac{\partial \eta}{\partial t} - 3\eta\frac{\dot{a}}{a^4} + \frac{\eta}{a^3}\dot{a}\nabla\mathbf{u} + \frac{\dot{a}\mathbf{u}}{a^3}\nabla\eta + 3\frac{\dot{a}}{a}\eta = 0$$

$$\Rightarrow \quad \frac{\mathrm{D}\eta}{\mathrm{D}t} + \eta\nabla\mathbf{u} = 0 \tag{2.5}$$

Finally, the Poisson equation becomes

$$\nabla^2\varphi = \frac{3\,t_0^2}{2\,a_0^3}\,\frac{3}{2}\,\dot{a}^2\delta = \frac{9\,t_0^2}{4\,a_0^3}\left(a_0\,\frac{1}{t_0^{2/3}}\,\frac{2}{3}\,t^{-1/3}\right)^2\delta = \left(a_0\,\frac{t^{2/3}}{t_0^{2/3}}\right)^{-1}\delta$$

$$\Rightarrow \quad \nabla^2\varphi = \frac{\delta}{a} \tag{2.6}$$

A formal solution of the continuity equation (2.5) can be immediately obtained by integration along the particle trajectory:

$$\eta(\mathbf{x}, a) = \eta_0(\mathbf{q})\exp\left[-\int_{a_0}^{a}\mathrm{d}a'\nabla\cdot\mathbf{u}(\mathbf{x}_{(\mathbf{q},a')}, a')\right]. \tag{2.7}$$

However, a more convenient form follows from the mass conservation of individual infinitesimal fluid elements that requires

$$\eta(\mathbf{x}, a)\mathrm{d}^3x = \eta_0(\mathbf{q})\mathrm{d}^3q,$$

where $\mathbf{q}$ is the initial Lagrangian position of the particle which has reached the Eulerian position $\mathbf{x}$ by the time $a(t)$, after all the Lagrangian-to-Eulerian transformation is nothing else than a coordinate change. Therefore one has the Lagrangian form

$$\eta(\mathbf{q}(\mathbf{x}, a), a) = \eta_0(\mathbf{q})\left|\left|\frac{\partial x}{\partial q}\right|\right|^{-1}, \tag{2.8}$$

where $\left|\left|\frac{\partial x}{\partial q}\right|\right|$ stands for the Jacobian determinant of the trasformation $x \to q$, or the Eulerian one

$$\eta(\mathbf{x}, a) = \eta_0(\mathbf{q})\left|\left|\frac{\partial q}{\partial x}\right|\right|, \tag{2.9}$$

which would require inverting the trajectory to find $\mathbf{q}(\mathbf{x}, a)$. These solutions are only valid as long as no shell-crossing has occurred, because otherwise the one-to-one correspondence between Lagrangian and Eulerian positions would be lost.

In spite of this limitation equation (2.7) has a relevant advantage compared to equation (2.8) or (2.9): it can be continued after the epoch of first shell-crossing to evaluate the density in the infinitesimal volume d^3x from those particles which were initially in d^3q.

2.1 The Zel'dovich approximation

The simplest approximation scheme is the linear one, which consist of neglecting the terms $(\mathbf{u}\cdot\nabla)\mathbf{u}$ in Euler equation and $\nabla\cdot(\delta\mathbf{u})$ in the continuity equation. Recall the results for the growing mode obtained in the previous chapter:

$$\delta \propto t^{\frac{2}{3}}, \qquad v' = av \propto t^{\frac{1}{3}}, \qquad \phi = \text{const}$$

therefore, in linear theory

$$\mathbf{u} = \frac{v}{\dot{a}} = \frac{v'}{a\dot{a}} \propto \frac{t^{\frac{1}{3}}}{t^{\frac{2}{3}}t^{-\frac{1}{3}}} \qquad \Rightarrow \qquad \mathbf{u} \approx \text{const}$$

$$\Rightarrow \quad \frac{\partial\,\mathbf{u}}{\partial a} = 0 \qquad \Rightarrow \qquad \frac{\mathrm{D}\mathbf{u}}{\mathrm{D}a} = 0 \tag{2.10}$$

hence, the velocity $\mathbf{u}$ can be expressed as the gradient of the potential $\mathbf{u} = -\nabla\varphi$. By substituting this result in the fluid equations we get

$$\begin{cases} \mathbf{u}_{LIN}(\mathbf{x},a) = -\nabla\varphi_0(\mathbf{x}) \\ \varphi_{LIN}(\mathbf{x},a) = \varphi_0(\mathbf{x}) \\ \eta_{LIN}(\mathbf{x},a) = 1 + a\nabla^2\varphi_0(\mathbf{x}) \end{cases}$$

The next step is the Zel'dovich approximation (ZEL) [3][4], which solution ansatz consist in extrapolating the validity of (2.10) even beyond linear theory. The justification is based on the fact that, in linear theory, going to Fourier space, recalling (1.14)and (1.13), we have:

$$\varphi_{\mathbf{k}} \propto \frac{\delta_{\mathbf{k}}}{k^2}, \qquad u_{\mathbf{k}} \propto k\varphi_{\mathbf{k}}$$

therefore the peculiar velocity $\mathbf{u}$, and even more so the peculiar gravitational potential $\varphi_{\mathbf{k}}$, keep on a linear level on smaller scales (i.e. longer times), than the density fluctuation field $\delta_{\mathbf{k}}$, because of the weights k^{-1} and k^{-2}.
We now have the following set of equations:

$$\begin{cases} \frac{\mathrm{D}\mathbf{u}}{\mathrm{D}a} = 0 \\ \\ \frac{\mathrm{D}\eta}{\mathrm{D}a} + \eta\nabla\cdot\mathbf{u} = 0 \end{cases} \tag{2.11}$$

Note that the Poisson equation has completely decoupled from the others and will be used only for initial conditions.
This system can be taken as the definition of ZEL , and it describes the dynamics of a set of collisionless particles (more precisely infinitesimal fluid elements) moving only under the effect of their inertia and preserving their mass. The solution of (2.10) is:

$$\mathbf{u}(\mathbf{x},a) = \mathbf{u}_0(\mathbf{q}) = -\nabla_{\mathbf{q}}\varphi_0(\mathbf{q}),$$

where $\mathbf{u}_0(\mathbf{q})$ is the initial ($a = a_0$) velocity in the Lagrangian position $\mathbf{q}$ of the fluid element which is the Eulerian position $\mathbf{x}$ at the time $a(t)$, therefore the velocity field is conserved along each particle trajectory.
We can further integrate to find the trajectory followed by a particle initially placed in $\mathbf{q}$, that is a straight line covered with constant speed $\mathbf{u}$ determined by the value of the initial peculiar gravitational potential in $\mathbf{q}$:

$$\mathbf{x}(\mathbf{q}, \tau) = \mathbf{q} - \tau \nabla_{\mathbf{q}} \varphi_0(\mathbf{q}),$$

with $\tau = a - a_0$; hence:

$$\mathbf{u}(\mathbf{x}(\mathbf{q}, a), a) = \mathbf{u}_0(\mathbf{q}) = \frac{\mathbf{x} - \mathbf{q}}{a}.$$

It is possible to define a velocity potential by $\mathbf{u}_{\mathrm{ZEL}}(\mathbf{x}, \tau) = \nabla_{\mathbf{x}} \Phi_{\mathrm{ZEL}}(\mathbf{x}, \tau) = \nabla_{\mathbf{q}} \Phi_0(\mathbf{q})$ ($\Phi = -\varphi$), which obeys the Hamilton-Jacobi equation:

$$\frac{\partial \Phi}{\partial \tau} + \frac{1}{2} \left(\nabla_{\mathbf{x}} \Phi\right)^2 = 0 \tag{2.12}$$

obtained by the substitution of $\mathbf{u} = \nabla_{\mathbf{x}} \Phi$ in the Euler equation (2.10), considering that

$$\begin{aligned} \frac{1}{2} \partial^i \Big(\partial_j \Phi \partial^j \Phi \Big) &= \partial^j \Phi \partial_i \partial_j \Phi = \partial^j \Phi \partial_j \partial_i \Phi \\ &= u^i \partial_j u^i \equiv \big(\mathbf{u} \cdot \nabla\big) \mathbf{u}. \end{aligned}$$

The integration of the Zel'dovich-Bernoulli equation (2.12), has been considered by Nusser and Dekel (1992) [5] to reconstruct the primordial density field from the present large-scale velocity or density field. The solution of (2.12) can be expressed as:

$$\Phi_{\mathrm{ZEL}}(\mathbf{x}, \tau) = \Phi_0(\mathbf{q}) + \frac{(\mathbf{x} - \mathbf{q})^2}{2\tau}.$$

We can represent the density field according to equation (2.8):

$$\eta_{\mathrm{ZEL}}(\mathbf{q}, \tau) = \eta_0(\mathbf{q}) \left|\left| \mathbf{1} + \tau D_0(\mathbf{q}) \right|\right|^{-1}, \tag{2.13}$$

here $\mathbf{1}$ is the unit matrix and D_0 is the deformation tensor, having components

$$D_{0,ij}(\mathbf{q}) = \frac{\partial^2 \Phi_0(\mathbf{q})}{\partial q_i \partial q_j}.$$

The deformation tensor can be locally diagonalized going to principal axes X_1, X_2, X_3, with eigenvalues λ_1, λ_2, λ_3. Thus we have:

$$\eta_{\mathrm{ZEL}}(\mathbf{q}, \tau) = \frac{\eta_0(\mathbf{q})}{[1 - \tau\lambda_1(\mathbf{q})][1 - \tau\lambda_2(\mathbf{q})][1 - \tau\lambda_3(\mathbf{q})]}. \tag{2.14}$$

According to the latter expression a singularity in Lagrangian space would form at every point $\mathbf{q}$ where at least one eigenvalue is positive; at the time $\tau_{\mathrm{SC}} = \lambda_i^{-1}$ the density will become

locally infinite. This event, called *shell-crossing*, is a consequence of the fact that when two (or more) particles coming from different Lagrangian positions $\mathbf{q}$, get to the same Eulerian position $\mathbf{x}$ at a certain time τ, the Jacobian $\left|\left|\frac{\partial x}{\partial q}\right|\right|$ is ill defined and diverges; the region where this happens is called *caustic*. A Lagrangian region where only one eigenvalue is positive will undergo a one-dimensional collapse along one axis to a *pankake* configuration, one where two eigenvalues are positive and one negative will collapse along two axis to a *filament*, and finally one for which all the eigenvalues are positive will collapse to a *knot*, or a *cluster-like* configuration.
According to Doroshkevich [7], if Φ_0 is a Gaussian random field (as predicted by inflation), there's a 42% probability for one positive and two negative eigenvalues and 42% for the opposite situation; in 8% of the cases all eigenvalues are positive and in the remaining 8% all eigenvalues are negative. Altogether there is a 92% probability that at least one eigenvalue is positive.
Besides being by construction consistent with the growing mode of linear perturbations at early times, ZEL provides a good approximation up to the time of firs shell-crossing.
The internal consistency of ZEL can be seen inserting the ansatz $\Phi = -\varphi$ into the Poisson equation, indeed one gets an alternative description for the density fluctuation

$$\nabla^2\varphi = \frac{\delta}{a} \qquad \Rightarrow \qquad \delta_{\mathrm{DYN}} = -a\nabla(\nabla\Phi) = -a\nabla\cdot\mathbf{u}\,,$$

which is nothing but the linear theory relation between peculiar velocity and density fluctuation. We refer to this expression of the density, $\eta_{\mathrm{DYN}} = 1 + \delta_{\mathrm{DYN}}$, as dynamical density to distinguish it from the continuity density obtained from equation (2.13) [6]. If we substitute this expression into the continuity equation, we get the mass density in Lagrangian form:

$$\eta_{\mathrm{DYN}}(\mathbf{q},\tau) = \frac{\eta_0(\mathbf{q})}{1-\tau\delta_+(\mathbf{q})} = \frac{\eta_0(\mathbf{q})}{1-\tau[\lambda_1(\mathbf{q})+\lambda_2(\mathbf{q})+\lambda_3(\mathbf{q})]}\,. \tag{2.15}$$

where we define the scaled initial growing mode $\delta_+ \equiv \frac{\delta_0}{a_0}$, which appears as the Poisson equation is used to relate φ_0 to δ_0. It is then clear that the Zel'dovich ansatz is only exact in one spatial dimension, or for one-dimensional perturbations, for in this case equations (2.14) and (2.15) coincide.
It has been proved bt Nusser et al. that the dynamical density contrast δ_{DYN} tends to overestimate the correct result, whereas δ_{ZEL} tends to underestimate it, hence the arithmetical mean $\frac{\delta_{\mathrm{DYN}}+\delta_{\mathrm{ZEL}}}{2}$ gives a better approximation of the actual value of δ.

From this discussion it is clear that the validity of the Zel'dovich approximation breakes down in case of caustic. Extending its validity after shell-crossing would imply that particles continue their motion along their straight trajectories, but this cannot be true since the gravitational interaction among neighbouring particles provides a stickening effect which is certainly going to modify their motion. The pankake configuratin will be stabilized by gravity and these two-dimensional configurations will happen to be the preferential sites for galaxy formation.

2.2 The frozen-flow approximation

We will now briefly intruduce the concepts behind the so called frozen-flow approximation [11], wherease a deeper discussion on its distinctive features and validity will be given in the following chapter.

This scheme allows an extrapolation beyond the time at which orbit-crossing would have occurred according to the Zel'dovich formulation. This is based on the idea of extrapolating the growing linear mode of the velocity field beyond its actual range of validity, while solving exactly the equation of continuity. Stream lines are then kept frozen to their initial shape, thus forcing the dynamics to remain in the laminar regime. Particles (or fluid elements) behave as massless tracers of the initial velocity field.

The frozen-fluid approximation (FFA) scheme starts with the linearized Euler equation (we neglect the term $(\mathbf{u}\cdot\nabla)\mathbf{u}$):

$$\frac{\partial \mathbf{u}}{\partial a} + \frac{3}{2a}\mathbf{u} = -\frac{3}{2a}\nabla\varphi_0\,,$$

where in the right-hand side the growing mode of the linear gravitational potential is assumed. This equation is solved by:

$$\mathbf{u}_{\rm FFA}(\mathbf{x},\tau) = \mathbf{u}_0(\mathbf{x}) = -\nabla_{\mathbf{x}}\varphi_0(\mathbf{x})\,, \tag{2.16}$$

remembering that τ was previously defined as $\tau = a - a_0$. In this approximation the peculiar velocity field $\mathbf{u}(\mathbf{x}, a)$ is frozen at each point to its initial value, so

$$\frac{\partial \mathbf{u}}{\partial \tau} = 0 \tag{2.17}$$

is valid, for it is the condition for steady flow. Either equation (2.16) or equation (2.17) can be used, toghether with continuity equation to define FFA. Particle trajectories can be described by the integral equation

$$\mathbf{x}(\mathbf{q},\tau) = \mathbf{q} - \int_0^\tau \mathrm{d}\tau'\,\nabla_{\mathbf{x}}\varphi_0\left[\mathbf{x}(\mathbf{q},\tau')\right]$$

that describes a motion during which the particles update their velocity at each infinitesimal step to the local value of the linear velocity field, without any memory of their previous motion, that is without inertia. This would be the case for a particle moving in a medium with a very large viscosity (in the friction dominated regime): the damping effect for the case we are dicussing, is determined by the Hubble drag, while the force is the gravitational one.
Also in this case, as it was for ZEL, a velocity potential can be defined: $\mathbf{u}_{\rm FFA}(\mathbf{x},\tau) = \nabla\Phi_{\rm FFA}(\mathbf{x},\tau)$, obeying the evolution equation:

$$\frac{\partial \Phi}{\partial \tau} = 0\,,$$

which is solved by

$$\Phi_{\rm FFA}(\mathbf{x},\tau) = \Phi_0(\mathbf{x}) = -\varphi_0(\mathbf{x})\,.$$

The velocity potential for both ZEL and FFA are equivalent up to the second order in the displacement ξ from the Lagrangian to the Eulerian position. In ZEL $\boldsymbol{\xi}$ is approximated by

$$\boldsymbol{\xi}_{\mathrm{ZEL}} = \tau \nabla_{\mathbf{q}} \Phi_0(\mathbf{q}) \,,$$

while in FFA it is approximated by

$$\boldsymbol{\xi}_{\mathrm{FFA}} = \int_0^\tau \mathrm{d}\tau' \, \nabla_{\mathbf{x}} \Phi_0[\mathbf{x}(\tau')] = \tau \nabla_{\mathbf{q}} \Phi_0(\mathbf{q}) + \mathcal{O}(\xi^2) \,.$$

We have:

$$\begin{aligned} \Phi_{\mathrm{FFA}}(\mathbf{x}, \tau) &= \Phi_0(\mathbf{x}) = \Phi_0(\mathbf{q} + \boldsymbol{\xi}) \\ &= \Phi_0(\mathbf{q}) + \nabla_{\mathbf{q}} \Phi_0(\mathbf{q}) \cdot \boldsymbol{\xi} + \frac{1}{2} \frac{\partial^2 \Phi_0(\mathbf{q})}{\partial q_i \partial q_j} \xi_i \xi_j + \mathcal{O}(\xi^2) \,, \end{aligned}$$

but it's easy to see that

$$\nabla_{\mathbf{q}} \Phi_0 = \frac{\boldsymbol{\xi}}{\tau} + \mathcal{O}(\xi^2) \,,$$

$$\frac{\partial^2 \Phi_0(\mathbf{q})}{\partial q_i \partial q_j} = -\frac{\delta_{ij}}{\tau} + \mathcal{O}(\xi),$$

therefore $\Phi_0(\mathbf{q} + \boldsymbol{\xi}) = \Phi_0(\mathbf{q}) + \frac{\xi^2}{2\tau} + \mathcal{O}(\xi^3)$, or

$$\Phi_{\mathrm{FFA}}(\mathbf{x}, \tau) = \Phi_{\mathrm{ZEL}}(\mathbf{x}, \tau) + \mathcal{O}(\xi^3) \,.$$

In order to complete the description, we need to find an expression for the density field: it can be driven from either equation (2.7) or (2.8) (or equivalently (2.9), for no caustics are formed at a finite time in FFA as we shall shortly see). Although all the expression for the density are interchangeable, it is interesting to write the comoving mass density as given by equation (2.7):

$$\eta_{\mathrm{FFA}}(\mathbf{x}, \tau) = \exp\left[\int_0^\tau \mathrm{d}\tau' \, \delta_+ \left[\mathbf{x}(\mathbf{q}, \tau') \right] \right] \,,$$

having assumed $\eta_0(\mathbf{x}_*) \approx 1$.
The logarithm of the density in $\mathbf{x}$ is given by the integral of the linear density field $\delta_+ \equiv \frac{\delta_0}{a_0}$ over the trajectory of the particle which has arrived in $\mathbf{x}$ at time τ, starting from the Lagrangian position $\mathbf{q}$. This result is quite different from the Lognormal Model bt Coles and Jones ([8], [9]) where η is assumed to be approximated by the exponential of the linear density field at the same Eulerian position. However, in both approximation, the non-linear density field tends to exponentiate the initial density fluctuation in the neighbourhood of high peaks. While this is only true for initial density peaks, it is a definite prediction for those points $\mathbf{x}_*$ that correspond to local maxima or minima for the initial velocity potential, that is great attractors or great repellers, in which case FFA yields:

$$\delta_{\mathrm{FFA}}(\mathbf{x}_*, \tau) = \exp\left[\delta_+(\mathbf{x}_*) \tau \right] - 1 \,.$$

Chapter 3

Understanding frozen-flow approximation

The physical motivations according to which we expect the frozen-flow approximation to work are connected to its consistency with the extrapolation of linear theory beyond its region of validity, to the possibility for the stream-lines to be curved instead of being exlusively straight and last, to the fact that around pankakes the particles slow down their motion, providing an artificial thickening that undertakes the role of gravitational interaction.
Now we will describe these motivations more in detail:

1. FFA is, by construction, consistent with linear theory, so it follows correctly the evolution at early times. The assumption of maintaining the linear approximation for the velocity potential even beyond the linear regime is justified by the fact that this quantity is more sensitive to large wavelenght modes that the density, and is therefore less affected by strongly non-linear evolution.

2. It is impossible for multi-stream regions to form, unless they were already present in the initial velocity field, since stream-lines are frozen to their initial shape. The frozen-flow approximation therefore avoids the formation of caustics at finite τ, so it is reasonable to try to extrapolate the approximation after the time at which the first shell-crossing would have appeared according to the Zel'dovich approximation.
   A particle moving according to FFA, has a null component of the velocity in a place where the same component for the initial gravitational force is zero; therefore it will slow down its motion along that direction approaching such a position: particles in FFA need infinite time to reach those places where a pankake, a filament or a knot will form. Moreover, since, unlike ZEL, these particles move along curved paths, as they come close to pancake configurations, they curve their trajectories, moving almost parallel to them; by doing so they try to reach the position of filaments, but as they cannot cross them, they modify their motion in order to approach asymptotically the filaments and to fall finally, for $\tau \to \infty$, into the knots corresponding to the minima of the initial gravitational potential.

3. This type of dynamics implies an artificial thickening of particles around pancakes, filaments and knots, which mimics the real gravitational clustering around these types of structures.

In order to analyse the latter point in more detail, we can consider a particle moving in the neighbourhood of some point $\mathbf{x}_*$, where the local deformation tensor, approximated by its initial value $D_{0,ij}(\mathbf{x}_*) = -\frac{\partial^2\varphi_0(\mathbf{x}_*)}{\partial x_i \partial x_j}$, has eigenvalues $\alpha_i \equiv \alpha_i(\mathbf{x}_*)$. Defining X_i as Cartesian coordinates along the principal axes af the local deformation tensor, with origin in $\mathbf{x}_*$, and $\xi_i \equiv X_i - \frac{1}{\alpha_i}\left.\frac{\partial\varphi_0}{\partial X_i}\right|_{\mathbf{x}_*}$, we have, at small distance from x_*:

$$\frac{\mathrm{d}^2\xi_i}{\mathrm{d}a^2} + \frac{3}{2a}\frac{\mathrm{d}\xi_i}{\mathrm{d}a} - \frac{3\alpha_i}{2a}\xi_i \approx 0\,, \qquad i = 1,2,3\,. \tag{3.1}$$

The second term in equation (3.1) plays the role of a time-dependent viscous force and it implies that the particle undergoes a damped motion along the ith axis. The FFA trajectory

$$\xi_i(\tau) = \xi_i(\tau)\, e^{\alpha_i \tau}\,,$$

provides a good approximation for the solution of (3.1) at early times, as long as the non-linear evolution of the peculiar gravitational potential can be neglected, therefore in this case it coincides with the growing mode of linear perturbations

$$\xi_i(\tau) = \xi_i(\tau)(1 + \alpha_i\tau)\,,$$

as the expansion of the exponential function returns the same behaviour. Moreover it also contains some qualitative features of the late-time behaviour, when the slowing down implied by the expansion of the Universe eventually dominates the overall dynamics, that is the damped motion due to the viscous term, becomes the most relevant component and so the first term in equation (3.1) is negligible.
The physical thickening of particle density around pancakes, filaments and knots, caused by damped oscillations around these structures, is here replaced by an approximately exponential slowing down of particle motions, which, however, overestimates the actual particle deceleration. By ascertaining this we come to the conclusion that FFA overshoots the actual dynamics.
Provided that we forgo the attempt to resolve the trajectories of individual particles, these effects produce a density field which looks similar to the real one; in this sense the method should be considered intrinsically Eulerian.

3.1 Validity of the method

The previously alleged reasons for the FFA to work powerfully can be better understood by applying both ZEL and FFA approximation to two models used to imprint different types of perturbations on an uniform background of particles, and then comparing the results obtained.

3.1.1 Toy model

The first model taken in consideration is a simple toy model, where the initial perturbation of the gravitational potential is obtained by the superposition of three sinusoids, one for each axis, each with a different amplitude and wavelength:

$$\varphi_0 = -\sum_{i=1}^{3} A_i \cos(k_i x_i)\,, \tag{3.2}$$

where we can take all the A_i to be positive. This perturbation generates a compensated cosine density enhancement at the centre of the perturbed area (for a more exhaustive dissertation on this topic see the work of Moutarde et al. (1991) [10]).

According to ZEL one has the following trajectories:

$$x_i(q_i,\tau) = q_i - \tau A_i k_i \sin(k_i x_i)\,, \qquad i = 1,2,3$$

and the Jacobian $\frac{\partial x}{\partial q}$ turns out to be diagonal, so, using (2.8), the density is immediately evaluated in the Lagrangian form:

$$\eta_{\mathrm{ZEL}}(\mathbf{q},\tau) = \prod_{i=1}^{3} \left[1 - \tau A_i k_i^2 \cos(k_i q_i)\right]^{-1},$$

where the initial density field $\eta_0(\mathbf{q}) \approx 1$, provided that $\delta_0 \approx 1$. Caustic forms where at least one component satisfies $\cos(k_i\tilde{q}_i) = \frac{1}{A_i k_i^2 \tau}$, for $\tau \geq \frac{1}{A_i k_i^2}$. The first shell-crossings appear at the time $\tau_{\mathrm{SC}} = \min\left(\frac{1}{A_i k_i^2}\right)$, at the Lagrangian positions $\tilde{q}_i = \pm\frac{2N\pi}{k_i}$ (with N=0, 1, 2, ...), since the cosine is equal to 1, corresponding to the Eulerian ones $\tilde{x}_i = \frac{\pm 2N\pi}{k_i}$.

The equation of motion according to FFA is:

$$\frac{\mathrm{d}x_i}{\mathrm{d}\tau} = -A_i k_i \sin(k_i x_i)\,, \qquad i = 1,2,3\,,$$

and is solved by:

$$\ln\left|\tan\frac{k_i x_i}{2}\right| = \ln\left|\tan\frac{k_i q_i}{2}\right| - A_i k_i^2 \tau\,.$$

The tangents change sign when the argument is a multiple of π, so when we have $x_i = \pm N\pi/k_i$ and $q_i = \pm N\pi/k_i$ (i=1, 2, 3; N=0, 1, 2, ...), but the particles with Lagrangian coordinates $q_i = \pm N\pi/k_i$ do not move along the ith direction, therefore each region bounded by $x_i = \pm N\pi/k_i$ evolves separately.
From the former equation we get:

$$x_i(q_i,\tau) = \frac{2}{k_i}\arctan\left[e^{-A_i k_i^2 \tau}\tan\left(\frac{k_i q_i}{2}\right)\right],$$

which can be explicitly invertet to obtain:

$$q_i(x_i,\tau) = \frac{2}{k_i}\arctan\left[e^{A_i k_i^2 \tau}\tan\left(\frac{k_i x_i}{2}\right)\right].$$

The transformation matrix $\frac{\partial q}{\partial v}$ is diagonal so, using (2.9), the density can be easily evaluated in the Eulerian form:

$$\eta_{\rm FFA}(\mathbf{x},\tau) = \prod_{i=i}^{3}\left[e^{A_i k_i^2\tau} - 2\sinh\left(A_i k_i^2\tau\right)\cos^2\left(\frac{k_i x_i}{2}\right)\right]^{-1} . \tag{3.3}$$

As $\tau \to \infty$ the comoving mass density goes to zero everywhere like $\exp\left[-\sum_i A_i k_i^2\tau\right]$, exept in those places where at least one of the coordinates is such that $x_i = \pm\frac{2N_i\pi}{k_i}$ (N_i =1, 2, ...). If this happens to be true only for one coordinate, say x_1, pancakes-like configurations appear in the neighbourhood of the planes $x_1 = \pm\frac{2N_1\pi}{k_1}$, where the density goes like

$$\eta \propto \exp[(A_1 k_1^2 - A_3 k_3^2 - A_3 k_3^2)\tau] .$$

In the same way, if this is simultaneusly true for two coordinates, say x_1 and x_2, filamentary configurations appear along the lines $x_1 = \pm 2N_1\pi/k_1$, $x_2 = \pm 2N_2\pi/k_2$, with the density going like

$$\eta \propto \exp[(A_1 k_1^2 + A_3 k_3^2 - A_3 k_3^2)\tau] .$$

Finally, cluster-like configurations appear around the points $x_i = \pm\frac{2N_i\pi}{k_i}$ i=1, 2, 3, where the density grows like

$$\eta \propto \exp\left(\sum_{i=1}^{3} A_i k_i^2\tau\right) .$$

In the general case one has different exponential-like time evolutions for collapse along the three axis, $\tau_i = \frac{1}{A_i k_i^2}$. In the symmetric case, where $A_1 k_1^2 = A_2 k_2^2 = A_3 k_3^2$, the density fluctuation around knots tends to

$$\delta_{\rm knots} \sim e^{\sqrt{\frac{3}{2}}\delta_+\tau} - 1 . \tag{3.4}$$

3.1.2 Spherical top-hat model

The second model analyzed is the spherical top-hat one, which consist of a spherically symmetric initial irregularity of constant amplitude δ_0 and radius R, included in an Einstein-de Sitter Universe. Inside the sphere the gradient of the initial gravitational potential is:

$$\frac{{\rm d}\varphi_0}{{\rm d}r} = \frac{\delta_+}{3} r , \tag{3.5}$$

where r stands for the radial coordinate comoving with respect to the background. The description can be semplified if $\delta_0 \ll 1$ (more precisely $a_0 \to 0$ at finite $\delta_+ = \frac{\delta_0}{a_0}$). Starting from the description of a curved space, the trajectory of a particle with initial comoving position r_0 can be expressed in the parametric form [6]:

$$r(r_0,\tau) = r_0\frac{\kappa}{2}\left(\frac{4}{3}\right)^{\frac{2}{3}}\frac{1-\mathcal{C}_\kappa(\vartheta)}{\left[\kappa\left(\vartheta - \mathcal{S}_\kappa(\vartheta)\right)\right]^{\frac{2}{3}}} ,$$

where $\kappa = 1$ or $\kappa = -1$ according to whether δ_+ is respectively positive or negative; $\mathcal{C}_\kappa$ and $\mathcal{S}_\kappa$ stand for cos and sin if $\kappa = 1$ or for cosh and sinh if $\kappa = -1$; the parameter ϑ is related to the proper time and so also to the time variable τ as follows

$$\tau = \left(\frac{3}{4}\right)^{\frac{2}{3}} \Delta^{-1} \left[\kappa \left(\vartheta - \mathcal{S}_\kappa(\vartheta)\right)\right]^{\frac{2}{3}} ,$$

where $\Delta = |\delta_+|$ if the Universe expansion is initially unperturbed, or $\Delta = \frac{5|\delta_+|}{3}$ if only the growing mode is initially present; the latter is the most interesting case as the growing mode is present, because it is the one that allows a comparison among the top-hat model description and ZEL or FFA.
The expression for the density fluctuation can be easily evaluated from the Jacobian determinant (2.9)

$$\left|\left|\frac{\partial q}{\partial x}\right|\right| = \left(\frac{r_0}{r}\right)^2 \frac{\mathrm{d}r_0}{\mathrm{d}r}$$

and remembering that $\delta = \eta - 1$:

$$\delta_{\mathrm{TH}}(\tau) = \frac{9\kappa \left(\vartheta - \mathcal{S}_\kappa(\vartheta)\right)^2}{2\left(1 - \mathcal{C}_\kappa(\vartheta)\right)^3} - 1 .$$

The same problem can be easily solved following ZEL, by starting from equation (3.5); particle trajectories read:

$$\mathbf{r}(\mathbf{r}_0, \tau) = \mathbf{r}_0 - \tau \left.\frac{\mathrm{d}\varphi_0}{\mathrm{d}r}\right|_{\mathbf{r}_0} = \mathbf{r}_0 \left(1 - \frac{\delta_+ \tau}{3}\right) ,$$

so that, using the Jacobian determinant, the density fluctuation is

$$\delta_{\mathrm{ZEL}}(\tau) = \left(1 - \frac{\delta_+ \tau}{3}\right)^{-3} - 1 .$$

According to FFA we have $\mathbf{u}(r, \tau) = \frac{\mathrm{d}\mathbf{r}}{\mathrm{d}\tau} = -\frac{\mathrm{d}\varphi_0}{\mathrm{d}r}$, therefore the evolution of particle trajectories can be easily evaluated by substituting in (3.5) the derivative of the gravitational potential:

$$\mathbf{r}(\mathbf{r}_0, \tau) = \mathbf{r}_0 \, e^{-\frac{\delta_+ \tau}{3}} .$$

The density fluctuation changes as

$$\delta_{\mathrm{FFA}}(\tau) = e^{\delta_+ \tau} - 1 ,$$

as it can be easily obtained from tha Jacobian determinant (note the similarity to (3.4)). At early times all previous expressions for δ consistently reduce to the growing linear mode $\delta_{\mathrm{LIN}} = \delta_+ \tau$.
A spherical perturbation of mass, initially contained inside a sphere of radius r_0, by time τ will be contained in a sphere of physical radius $r_{\mathrm{ph}}(r_0, \tau) = \tau \, r(r_0, \tau)$. As it can be easily seen, for $\delta_+ < 0$ the sphere expands forever, while for $\delta_+ > 0$ it expands up to a specific time

of turnaround, $\tau_{\rm ta}$, when it reaches its maximum size: $r_{\rm ph}(\tau_{\rm ta}) = \frac{3r_0}{e\delta_+}$, after which it collapses by self-gravity, making the central density becoming infinite at $\tau_{\rm coll}$.
The overdensity at turnaround $\delta_{\rm ta}$ is a useful parameter, since it is independent both from the amplitude of the initial overdensity δ_+ and form the initial conditions on the peculiar velocity field. We will now compare the results for the exact top-hat model, where the turnaround corresponds to $\vartheta = \pi$, ZEL and FFA:

Table 3.1: Obtained results

T-H	ZEL	FFA
$\tau_{\rm ta} = \left(\frac{3\pi}{4}\right)^{\frac{2}{3}} \Delta^{-1}$	$\tau_{\rm ta} = \frac{3}{2}\delta_+$	$\tau_{\rm ta} = \frac{3}{\delta_+}$
$r_{\rm ph}(\tau_{\rm ta}) = r_0\Delta^{-1}$	$r_{\rm ph}(\tau_{\rm ta}) = \frac{3r_0}{4\delta_+}$	$r_{\rm ph}(\tau_{\rm ta}) = \frac{3r_0}{e\delta_+}$
$\delta_{\rm ta} = \left(\frac{3\pi}{4}\right)^2 - 1$	$\delta_{\rm ta} = 7$	$\delta_{\rm ta} = e^3 - 1$
$\tau_{\rm coll} = \left(\frac{3\pi}{2}\right)^{\frac{2}{3}} \Delta^{-1}$	$\tau_{\rm coll} = 2\tau_{\rm ta}$	$\tau_{\rm coll} \to \infty$

The overdensity turnaround for FFA reads $\delta_{\rm ta} = e^3 - 1$, which overestimates the correct value by a factor of ≈ 4.
A plot of the density contrast obtained from FFA, ZEL and the linear theory (LIN), versus the exact solution, is shown in figure 3.1.

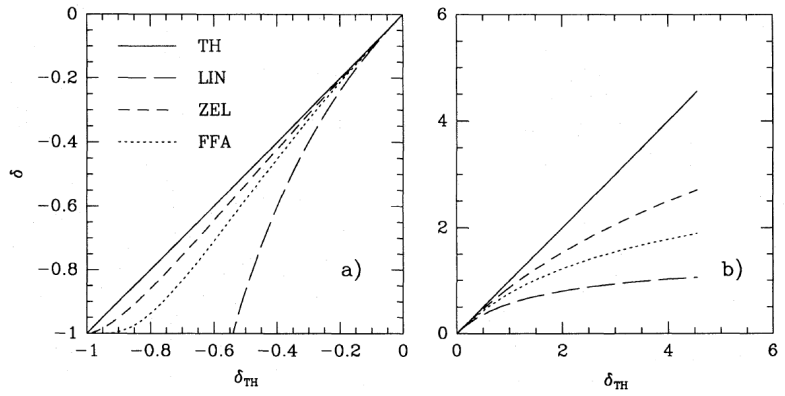

Figure 3.1: Figure taken from [11].

In FFA, for a positive density perturbation, each particle is exponentially decelered while approaching $r = 0$, therefore the resulting density enhancement turns out to be always underestimated; this feature, however, is strictly related to the impossibility of caustic formation. For a negative perturbation, instead, FFA overshoots the expansion of the void, as we have already pointed out in the beginnin of this section.

3.2 Large-scale structure evolution

Now that we have built our approximation schemes we can compare the results obtained by applying FFA, ZEL and a N-body simulation on the evolution of structures on large scales.

In order to make this comparison we can use numerically evolved simulations with 64^3 particles on a cubic grid, where the particles were initially uniformly distributed. An initial redshift $z_0 = 18$ was chosen. The particles were moved according to ZEL and FFA up to the present time $z = 0$ and the results were compared to the ones obtained by an N-body simulation (results taken from [11]).

Figure 3.2 shows projected particle positions in slices of depth 1000 km s^{-1} at the present time (z= 0), all drawn from the same initial conditions. Compared to the N-body simulation in figure 3.2a, the results of FFA, figure 3.2b, recover all the main structures in the correct places, even though they appear to be thicker and the voids are more empty and conspicuous. FFA leads to an excess of substructure, wich is carried on during the evolution instead of being erased by the hierarchical clustering process as it would have happened in the true dynamics; this aspect of the non linear evolution is very clearly exposed by the numerical experiments of Little; Weinberg & Park (1991)[12].

The structures obtained by the Zel'dovich approximation in figure 3.2c, instead, are less prominent and more fuzzy, since the particles have diffused away from the caustic positions after shell-crossing.

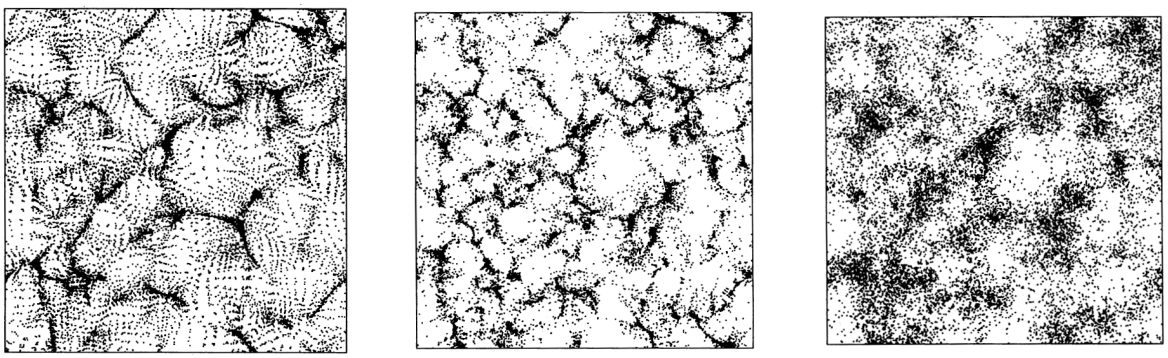

(a) PM (b) FFA (c) ZEL

Figure 3.2: Figure taken from [11].

In figure 3.3 the smooth density for 1000 randomly selected grid points is plotted for FFA and ZEL versus the corresponding N-body density, et redshifts $z = 0.5$ and $z = 0$. Compared to ZEL, FFA shows results that are more scattered around the N-body values, but do not show the systematic underestimate for low and for high δ values: the density fluctuation values are more evenly distributed around the N-body line, furthermore the time evolution and/or the the increased resolution amplify the features discussed above.

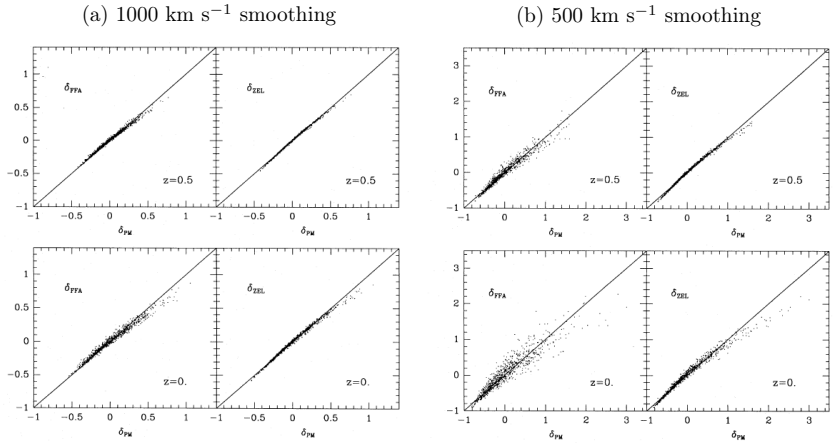

Figure 3.3: Figure taken from [11].

A complementary way to analyse these results is to take in consideration isodensity contours (presented at z=0), as displayed in figure 3.4a in a slice with thickness 500 km s^{-1}, smoothed with a Gaussian filter of radius 1000 km s^{-1} (left) and 500 km s^{-1} (right). In the isodensity representation thick line marks $\delta = 0$, solid lines $\delta > 0$ and dashed lines negative ones. The FFA simulation provides a more accurate representation of the regions of highest and lowest density.

Figure 3.4: Figure taken from [11].

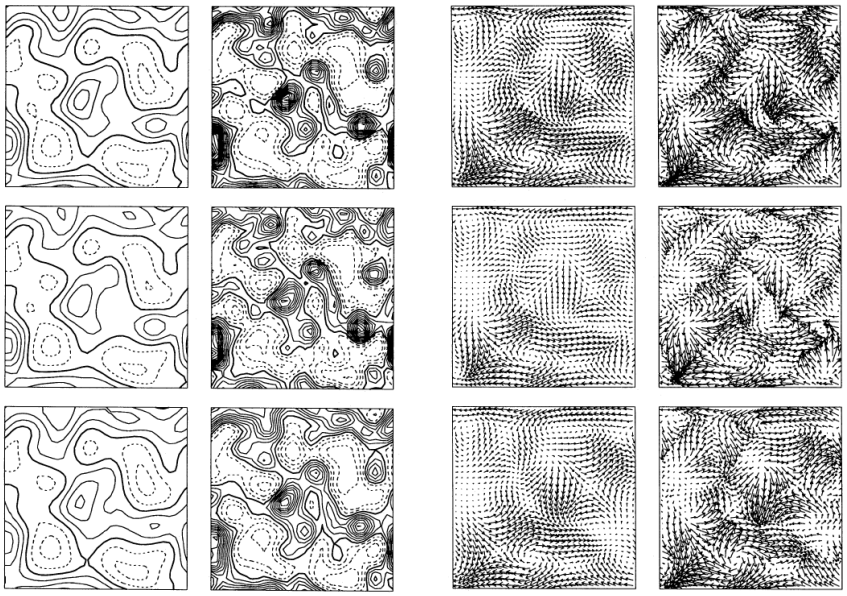

(a) Filtered density contrast for the N-body simulation (top), FFA (center) and ZEL (bottom).

(b) Filtered peculiar velocity field for the N-body simulation (top), FFA (center) and ZEL (bottom).

A further comparison can be done using the peculiar velocity field, showed in figure 3.4b for the same slices as in figure 3.4a. The FFA result is just the linear velocity field: it traces reasonably well the evolution simply because the velocity field gives larger weight to small wavenumbers than the density fluctuation field does.

The previous results suggest that FFA is able to reproduce the mass density distribution more accurately than ZEL. One can check this by considering cell-count statistics, counting the number N of particles inside cubic boxes with varying sides R_b =250, 500, 1000 km s^{-1}. The cell-count distribution $P(N)$ is shown in figure 3.5 at two times $z = 0.5$ and 0.

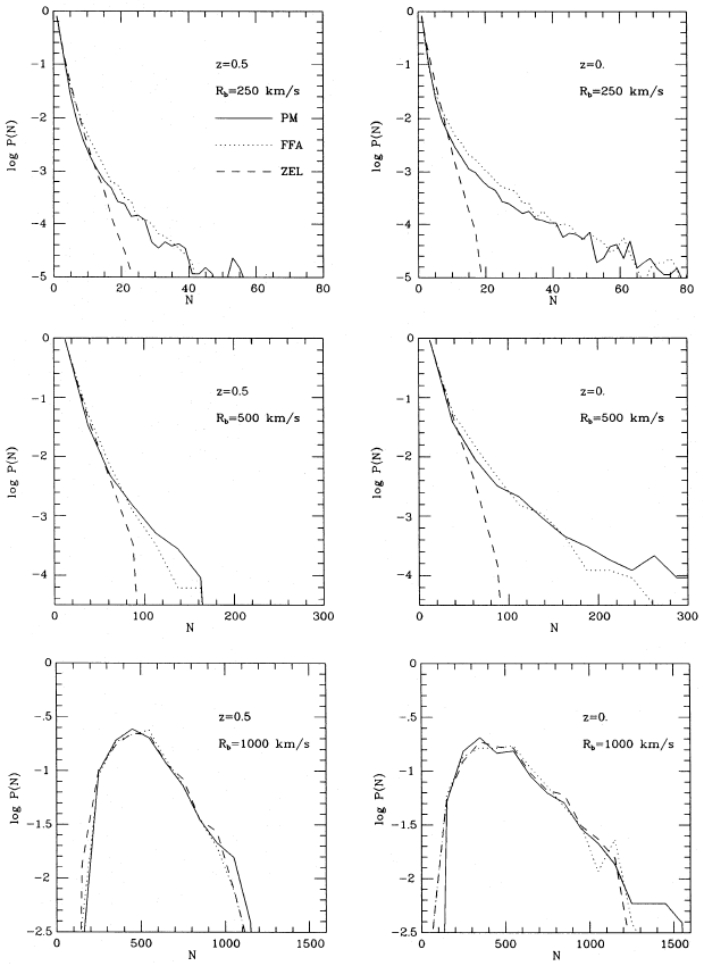

Figure 3.5: Figure taken from [11].

Even though the initial conditions are Gaussian, the clustering dynamics, which is assumed to be accurately described by the N-body curve, produce a skew-positive distribution. Unlike ZEL, FFA mimics reasonably well the long high-N tail; the two approximations become equivalent and similar to the N-body results when the largest box size is used. The advantages of FFA become more evident when small scales and late times are considered.

Chapter 4

Beyond frozen-flow approximation

The simple model for the evolution of structures described so far, assumes that the velocity potential is linearly related at any time to the local value of the initial gravitational potential. Therefore using this description we disregard the non-linear effects caused by the back-reaction of the evolving mass density on the peculiar velocity field itself, as particles behave as its massless tracers.

This would result in some physical processes such as merging of pancakes, which frozen-flow approximation cannot describe. In fact figure 3.2 shows that the results obtained by FFA and ZEL differ from the true non-linear dynamics, displayed by the N-body simulation, mainly because of the lack of merging of structures. One can try to improve the approximation scheme by considering an 'artificial' evolution of the velocity potential in the manner of the adhesion model.

4.1 Adhesion model

The adhesion model [13] tries to overcome the limitations of the Zel'dovich approximation by adding an artificial viscosity term to Euler equation (2.10), which can thus be replaced by:

$$\frac{\mathrm{D}\mathbf{u}}{\mathrm{D}\tau} = \nu \nabla^2 \mathbf{u}\,, \tag{4.1}$$

having defined $\tau \equiv a(t)$. This kinematical viscosity term mimics the actual sticking of particles around pancakes, caused by the action of gravity even in a collisionless medium, and is such that its effect is large close to the sites of possible shell-crossing and negligible otherwise. The parameter ν plays the role of a coefficient of kinematical viscosity which controls the thickness of pancakes.

The previous equation is the vector generalization of the *Burgers equation* [14] and it can be solved by assuming in the first place that the flow is irrotational, therefore the velocity can be expressed as the gradient of a potential field:

$$\mathbf{u}_{\mathrm{ADM}} = \nabla \Phi_{\mathrm{ADM}}$$

using this relation and starting from (4.1) one obtains the Bernulli equation:

$$\frac{\partial \Phi}{\partial \tau} + \frac{1}{2}\left(\nabla \Phi\right)^2 = \nu \nabla^2 \Phi \,.$$

Going into detail, it is known that Burgers equation can be analitically solved through the non-linear *Hopf-Cole transformation*:

$$\Phi = -2\nu \ln \mathcal{U} \,, \tag{4.2}$$

where $\mathcal{U}$ has an exponential behaviour. By replacing (4.2) in the Bernulli equation one gets the *Fokker-Planck equation*:

$$\frac{\partial \mathcal{U}}{\partial \tau} = \nu \, \nabla^2 \mathcal{U} \,, \tag{4.3}$$

known also as linear diffusion equation. It is a parabolic linear differential equation that needs both initial and boundary conditions to be solved. If we consider a trial solution of the form

$$\mathcal{U}(\mathbf{x}, \tau) = f(\tau) g(\mathbf{x}) \,,$$

and we solve by separating the variables we get:

$$f(\tau) = e^{\mathcal{E}\tau} \,, \qquad \mathcal{E} g(\mathbf{x}) = \nu \, \nabla^2 g(\mathbf{x}) \,,$$

going to Fourier space the latter expression reads:

$$\mathcal{E}_k g_{\mathbf{k}} = -\nu k^2 g_{\mathbf{k}} \quad \Rightarrow \quad \mathcal{E}_k = -\nu k^2 .$$

Applying the superposition principle, the general solution becomes:

$$\mathcal{U}(\mathbf{x}, \tau) = \int \frac{\mathrm{d}^3 k}{(2\pi)^3} \, e^{-\nu k^2 \tau} \, g_{\mathbf{k}} \, e^{i \mathbf{k} \cdot \mathbf{x}} \tag{4.4}$$

where $g_{\mathbf{k}}$ are some generic coefficents which have to be determined by the initial and boundary conditions.
The expression for the required $\mathcal{U}$, corresponding to the fixed initial conditions $\mathcal{U}_0(\mathbf{q})$, can be obtained by considering the *kernel* of the solutions, which, in the diffusion process interpretation, expresses the probability that a particle can be found in $\mathbf{x}$ at the time τ, given that it was in $\mathbf{q}$ at $\tau = 0$. Therefore for $\tau \to 0$, the kernel coincides with the solution corresponding to a *Dirac delta function*:

$$\mathcal{K}(\mathbf{x}, \tau | \mathbf{q}, 0) \underset{\tau \to 0}{\longrightarrow} \delta(\mathbf{x} - \mathbf{q}) \,.$$

Since the general solution (4.4) has to be a Dirac delta function for $\tau = 0$, we have to impose the generic coefficents $g_{\mathbf{k}}$ to be $g_{\mathbf{k}} = e^{-i\mathbf{k}\mathbf{q}}$ in order to obtain this result

$$\mathcal{K}(\mathbf{x}, \tau | \mathbf{q}, 0) = \int \frac{\mathrm{d}^3 k}{(2\pi)^3} \, e^{-\nu k^2 \tau} \, e^{i \mathbf{k} (\mathbf{x} - \mathbf{q})} \underset{\tau \to 0}{\longrightarrow} \delta(\mathbf{x} - \mathbf{q}) \,.$$

The integral expression above can be easily solved multiplying and dividing by a factor $e^{\frac{(\mathbf{x}-\mathbf{q})^2}{4\nu\tau}}$, then one gets:

$$\mathcal{K}(\mathbf{x},\tau|\mathbf{q},0) = (4\pi\nu\tau)^{-\frac{3}{2}}\, e^{-\frac{(\mathbf{x}-\mathbf{q})^2}{4\nu\tau}}\,,$$

that is a *Gaussian probability distribution* centered in $\mathbf{q}$, with dispersion $2\nu\tau$ which increases with time.
We have previously seen that the kernel of the solutions assumes the meaning of a conditional probability, therefore if we recall *Bayes theorem*, which states that that the conditional probability of an event A given that the event B has happened is equal to the ratio between the joint probability of A and B and the probability of B:

$$P(A|B) = \frac{P(A,B)}{P(B)}\,,$$

remembering that $P(A) \equiv \int \mathrm{d}B P(A,B)$ and so that:

$$P(A) = \int \mathrm{d}B P(B) P(A|B), \tag{4.5}$$

we get the required $\mathcal{U}$ corresponding to our initial conditions $\mathcal{U}_0(\mathbf{q})$ using a merely reformulation of (4.5), the *Chapman-Kolmogorov equation*:

$$\mathcal{U}(\mathbf{x},\tau) = \int \mathrm{d}^3q\, \mathcal{U}_0(\mathbf{q})\, \mathcal{K}(\mathbf{x},\tau|\mathbf{q},0)\,. \tag{4.6}$$

Because of the definition of $\mathcal{U}$, given by the transformation (4.2), and recalling that $\mathbf{u}_0(\mathbf{q}) = -\nabla_q \varphi_0(\mathbf{q})$, we have:

$$\mathcal{U}_0(\mathbf{q}) = e^{-\frac{\Phi_0(\mathbf{q})}{2\nu}} = e^{\frac{\varphi_0}{2\nu}}\,,$$

substituting it in (4.6) we get:

$$\mathcal{U}(\mathbf{x},\tau) = \int \frac{\mathrm{d}^3q}{(4\pi\nu\tau)^{3/2}}\, e^{-\frac{S(\mathbf{x},\mathbf{q},\tau)}{2\nu}}\,,$$

where we have defined the action S as: $S(\mathbf{x},\mathbf{q},\tau) = \frac{(\mathbf{x}-\mathbf{q})^2}{2\tau} - \varphi_0(\mathbf{q})$, which satisfies the free Bernoulli equation with $\nu = 0$ (Hamilton-Jacobi):

$$\frac{\partial S}{\partial \tau} + \frac{1}{2}\left(\nabla S\right)^2 = 0\,.$$

The velocity field reads:

$$\mathbf{u}_{\mathrm{ADM}}(\mathbf{x},\tau) = -2\nu\frac{\nabla\mathcal{U}}{\mathcal{U}} = \frac{\int \mathrm{d}^3q\, \left(\frac{\mathbf{x}-\mathbf{q}}{\tau}\right) e^{-\frac{S(\mathbf{x},\mathbf{q},\tau)}{2\nu}}}{\int \mathrm{d}^3q\, e^{-\frac{S(\mathbf{x},\mathbf{q},\tau)}{2\nu}}}\,.$$

The Eulerian positions are then found by direct integration [15], [16]:

$$\mathbf{x}(\mathbf{q},\tau) = \mathbf{q} + \int_0^\tau \mathrm{d}\tau'\, \mathbf{u}_{\mathrm{ADM}}[\mathbf{x}(\mathbf{q},\tau'),\tau']\,,$$

while the density field can be obtained recalling equation (2.9):

$$\eta(\mathbf{x},\tau) = \left|\left|\frac{\partial q}{\partial x}\right|\right| .$$

The coefficent ν regulates the thickness of our artificial pancakes, which is proportional (by dimentional arguments) to $\nu^{1/2}$. We are interested in small values of ν, formally in the $\nu \to 0$ limit (for which ZEL is re-obtained), which correspons to the limit of large Reynolds number $\mathscr{R}_0 = \frac{u_0 \ell_0}{\nu}$, where u_0 and ℓ_0 are the amplitude and scale of the initial velocity field. In such a limit one can evaluate the integral over $\mathbf{q}$ using the *steepest-discent*, or *saddle point* approximation.
This is based on the idea that for our sharply peaked function $e^{-\frac{S}{2\nu}}$ the largest contribution to the integral comes from the absolute minima $\mathbf{q}_s$ of $S(\mathbf{x},\mathbf{q},\tau)$, for given $\mathbf{x}$ and τ, satisfying $\nabla_q S(\mathbf{x},\mathbf{q},\tau)|_{\mathbf{q}_s} = 0$. We therefore expand S to second order around these minima:

$$\begin{aligned}\mathcal{U}(\mathbf{x},\tau) &= (4\pi\nu\tau)^{-\frac{3}{2}} e^{-\frac{S(\mathbf{x},\mathbf{q}_s,\tau)}{2\nu}} \int \mathrm{d}^3 q \exp\Big[-\frac{1}{4\nu} \sum_{i,j=1}^{3} \frac{\partial^2 S}{\partial q_i \partial q_j}\Big|_{\mathbf{q}_s} \delta q_i \delta q_j \Big] \\ &= e^{-\frac{S(\mathbf{x},\mathbf{q}_s,\tau)}{2\nu}} \sum_s j_s(\mathbf{x},\mathbf{q}_s,\tau) ,\end{aligned}$$

where

$$j_s(\mathbf{x},\mathbf{q}_s,\tau) = \left(\det \left[\frac{\partial^2 S(\mathbf{x},\mathbf{q},\tau)}{\partial q_i \partial q_j} \right]_{\mathbf{q}_s} \right)^{-\frac{1}{2}} .$$

We then obtain:

$$\mathbf{u}(\mathbf{x},\tau) = \sum_s \frac{\mathbf{x}-\mathbf{q}_s}{\tau} w_s(\mathbf{x},\mathbf{q}_s,\tau) , \qquad w_s \equiv \frac{j_s}{\sum_s j_s} ,$$

having used the fact that

$$\frac{\mathbf{x}-\mathbf{q}_s}{\tau} = \nabla_q S(\mathbf{x},\mathbf{q}_s,\tau)$$

and that the function $S(\mathbf{x},\mathbf{q}_s,\tau)$ has to be the same in all the absolute minima. In summary we have found that the velocity takes contribution from different trajectories starting from the absolute minima $\mathbf{q}_s$ of S for given $\mathbf{x}$ and τ.

This model allows one to obtain the skeleton of the large-scale matter distribution by a geometrical technique based on the insertion of osculating paraboloids into the hypersurfaces of the initial velocity potential or of the initial linear gravitational potential, provided that crossings are not allowed. The advantage of this model is that the skeleton of the large-scale structures can be found at an arbitrary time with no consideration of previous evolution, since the time is involved in the result only as a parameter determining the curvature of the paraboloid.

The results of the N-body simulation and the adhesion model can be compared (for pure power-law initial spectra with several indices, $n = -2,\ 0,\ +2$) by displaying the particle positions and the skeleton of the structure for the same initial conditions and the same moment in the same figure, as done in the work of Kofman et al. (1992) [17]. For the values $n = -2$

and $n = 0$ simulations show a very good visual agreement between the skeleton and the particle distribution in N-body simulations. Good agreement for these simulations was found for the all moments studied. There is not such good agreement for the $n = 2$ simulation for the moment shown in figure 4.1.

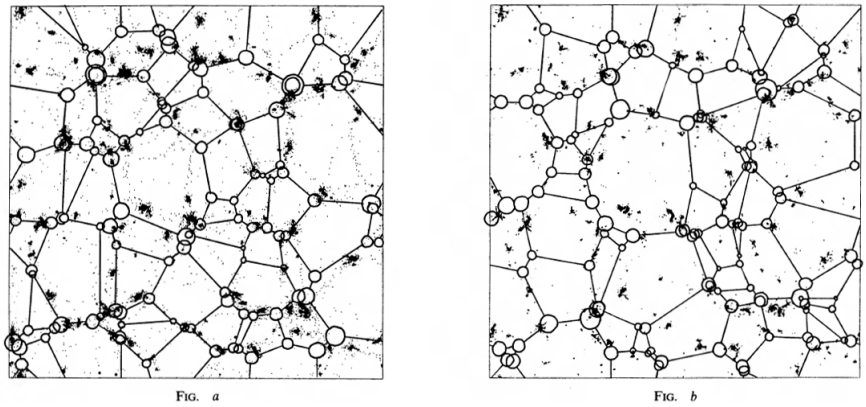

Figure 4.1: In (a) $n = 2$, moment $k = 32$, epoch $\sigma = 62.7$. In (b) $n = 2$, moment $k = 256$, epoch $\sigma = 4031$. Figure taken from [17].

To find the reason why the adhesion model does not work so well beginning from some critical moment, as happens in the $n = 2$ simulation, we need to better understand structure formation. At late times, when the skeleton of the structure is determined by the large-scale part of the potential, it can be represented by the sum of the initial potential and an additional part due to non-linear evolution. This extra part of the potential is generated by the local gravity of non-linear clumps.
If the typical scale of the non-linear evolution is smaller than the scale of significant correlation of the initial potential then we expect that coherent initial motion is disturbed only a little by the local gravity. At still later times, the characteristic scale of the structure exceeds the scale of the initial potential, and local gravity dominates the motion.

4.2 Viscid-flow approximation

Since, as we have seen in the previous paragraph, the adhesion model fails from some critical moment, we can try to develop an alternative method starting from FFA instead of ZEL.

Following the idea behind the adhesion model, we can modify FFA by adding an artificial viscosity term to the right side of the equation (2.17):

$$\frac{\partial \mathbf{u}}{\partial \tau} = \nu \nabla^2 \mathbf{u}$$

and similarly for the velocity potential:

$$\frac{\partial \Phi}{\partial \tau} = \nu \nabla^2 \Phi \,.$$

We shall refer to this model as the viscid-flow approximation (VFA). The problem is then reduced to the solution of the linear diffusion equation, which yields:

$$\Phi_{\rm VFA}(\mathbf{x},\tau) = \frac{1}{(4\pi\nu\tau)^{\frac{3}{2}}} \int {\rm d}^3q\, \Phi_0(\mathbf{q})\, e^{-\frac{(\mathbf{x}-\mathbf{q})^2}{4\nu\tau}} \tag{4.7}$$

and, for the velocity components,

$$\mathbf{u}_{\rm VFA}(\mathbf{x},\tau) = \frac{1}{(4\pi\nu\tau)^{\frac{3}{2}}} \int {\rm d}^3q\, \frac{\mathbf{x}-\mathbf{q}}{\tau}\, \Phi_0(\mathbf{q})\, e^{-\frac{(\mathbf{x}-\mathbf{q})^2}{4\nu\tau}}\,. \tag{4.8}$$

It is immediately clear that these solutions and the corresponding equations can be obtained from Burgers' theory in the limit of small Reynolds numbers, $\Phi_0 \ll 2\nu$ (or in the $\nu \to \infty$ limit at fixed $\nu\tau$). This fact connects ADM to VFA and, indirectly, ZEL to FFA: the Zel'dovich algorithm corresponds to the $\mathscr{R}_0 \to \infty$ limit of the adhesion model, whilst $\mathscr{R}_0 \ll 1$ yelds the viscid-flow approximation from which the frozen-flow one is finally obtained for $\nu \to 0$. The physical meaning of equations (4.7) and (4.8) is evident: the time evolution acts as a smoothing on the velocity field erasing small-scale motions; the time evolution has the effect of freezing the dynamics on larger and larger scales. These points become more clear using the expression of velocity potential in Fourier space:

$$\hat{\Phi}_{\rm VFA}(\mathbf{k},\tau) = \hat{\Phi}_0(\mathbf{k})\, e^{-k^2\nu\tau}\,.$$

If the initial velocity potential does not contain contributions on scales smaller than a certain cut-off wavenumber $k_{\rm min}$, the dynamics will be completely frozen and the Universe will enter a stationary regime after a time $\tau \sim \frac{1}{\nu k_{\rm min}}$.

These properties can be analysed in detail by considering the toy model discussed previously, according to which one has:

$$\Phi_{\rm VFA}(\mathbf{x},\tau) = \sum_{i=1}^{3} A_i \cos(k_i x_i) e^{-k_i^2\nu\tau}\,,$$

and

$$x_i(q_i,\tau) = \frac{2}{k_i} \arctan\left(e^{-A_i f_i(\tau)} \tan\frac{k_i q_i}{2}\right)\,,$$

where $f_i(\tau) \equiv \nu^{-1}(1-e^{-k^2\nu\tau})$. The density is

$$\eta_{\rm VFA}(\mathbf{x},\tau) \sim \prod_{i=1}^{3} \frac{1}{e^{\frac{A_i}{\nu}} - 2\sinh(\frac{A_i}{\nu})\cos^2\frac{k_i x_i}{2}}\,.$$

Pancakes, filaments and knots will form, in the same positions as those obtained for FFA applied to the toy model, whose density and thickness are now monitored by the value of the viscosity coefficient ν. As in the adhesion model, the physically relevant case is for small ν, because only in this case the thickness of pancakes becomes negligible compared to their relative distance. Moreover, this is the condition for having an appreciable overdensity within

this configurations. A high value of ν would imply a premature freezing of the dynamics before the actual non-linear collapse could start.

To test the behaviour of the approximations discussed, a one-dimensional toy model, obtained from equation (3.2) in the specific case $A_2 = A_3 = 0$, has been evolved according to ZEL, FFA and VFA. The normalization is such that a caustic forms in $x = q = 0$ at $\tau = 1$. In figure 4.2 is shown the comparison of the results for the Zel'dovich approximation (solid line), frozen-flow approximation (dashed line) and viscid-flow approximation with $\nu = 0.4$ (dotted line) in a single sin-wave model (our toy model). The quantities compared are the Eulerian versus Lagrange position, the Eulerian velocity and the density profile at three expansion times, $\tau = 0.95$, 1.5 and 3.

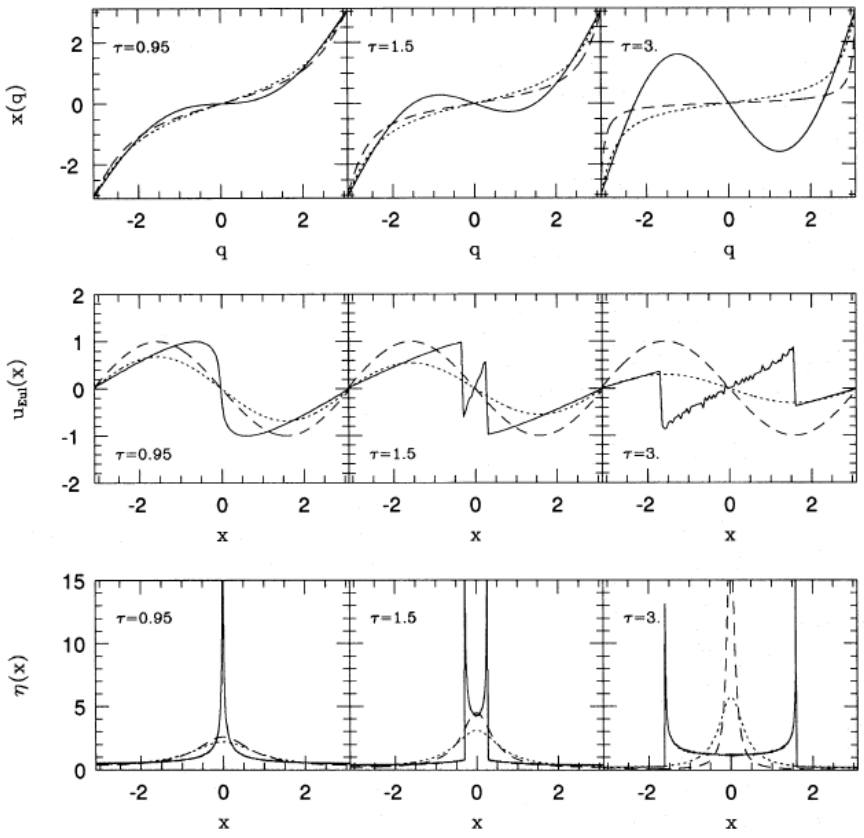

Figure 4.2: Figure taken from [11].

As it can be easily seen from the graphic, VFA provides the best approximation to the true Eulerian velocity field which, in the presence of multistream regions, corresponds to the algebraic sum of the three velocities, this suggests that VFA indeed provides an improvement over FFA

Conclusion

In this work we have discussed the issue of reconstructing the initial conditions of the clustering process, trying to overcome the problems arised by the particles shell-crossing. In this instance we have analysed the frozen-flow approximation to follow the non-linear dynamics of large-scale structures in a collisionless medium.

The method is based on solving the continuity equation exactly while extrapolating the linear approximation for the peculiar velocity field beyond its actual range of validity. This assumption allows one to prevent the occurence of orbit crossing, which represents the main drawback of the well known Zel'dovich approximation. Thanks to this property one is able to give a description of the Eulerian density field at later times and/or on smaller scales compared to the classical Zel'dovich algorhitm.

An important advantage of this method over more advanced techniques, such as the adhesion model or a full N-body code, is a strong reduction in the computational time, without a significant loss of accuracy. Therefore it could be applied to obtain fast simulations of the evolution of structures in the Universe on a wider range of scales and with a larger number of particles. Moreover frozen-flow approximation could be a reliable tool in reconstruction procedures of the initial density field from present-day data.

In addition frozen-flow approximation can be implemented in order to construct a method which follows the logic of the adhesion model: the viscid-flow approximation, that consists in adding an artificial viscosity term to the condition of steady flow. This technique overcomes the problems showed by the adhesion model in the simulations analysed by Kofman et al., providing a better approximation to the true Eulerian velocity field.

Bibliography

[1] P. P. Coles and F. Lucchin, "Cosmology", Wiley, 2002.

[2] S. Matarrese, “Notes on gravitational instability”, 2002–2005.

[3] Ya. B. Zel’dovich, “Fragmentation of a homogeneous medium under the action of gravitation”, *Astrophysics*, Vol. 6, pp. 164 -174, 1970.

[4] Ya. B. Zel’dovich, “Gravitational instability: an approximate theory for large density perturbations”, *Astronomy and Astrophysics*, Vol. 5, pp. 84-89, 1970

[5] A. Nusser, A. Dekel, "Tracing large-scale fluctuations back in time", *The Astrophysical Journal*, Vol. 391, pp. 443-452, Jun. 1992.

[6] A. Nusser, A. Dekel, E. Bertschinger, G. R. Blumenthal "Cosmological velocity-density relation in the quasi-linear regime", *The Astrophysical Journal*, Vol. 379, pp. 6-18, Sep. 1991.

[7] A. G. Doroshkevich, "Spatial structure of perturbations and origin of galactic rotation in fluctuation theory", *Astrophysics*, Vol. 6, p. 320-330, 1970.

[8] P. Coles, B. Jones, "A lognormal model for the cosmological mass distribution", *Monthly Notices of the Royal Astronomical Society*, Vol. 248, pp. 1-13, 1990.

[9] P. Coles, A. L. Melott, S. F. Shandarin, Testing approximations for non-linear gravitational clustering, *Monthly Notices of the Royal Astronomical Society*, Vol. 260, no. 4, pp. 765-776, 1992.

[10] F. Moutarde, J.M. Alimi, F. R. Bouchet, R. Pellat, A. Ramani, "Precollapse scale invariance in gravitational instability", *The Astrophysical Journal*, Vol. 382, pp. 377-381, Dec. 1991.

[11] S. Matarrese, F. Lucchin, L. Moscardini, D. Saez, “A frozen-flow approximation to the evolution of large-scale structures in the Universe”, *Monthly Notices of the Royal Astronomical Society*, Vol. 259, pp. 437-452, 1992.

[12] B. Little, D. H. Weinberg, C. Park, "Primordial fluctuations and non-linear structure", *Monthly Notices of the Royal Astronomical Society*, Vol. 253, pp. 295-306, 1991

[13] S. N. Gurbatov, A. I. Saichev, S. F. Shandarin, *Soviet Physic Dokl.*, 1985.

[14] J. M. Burgers, "The non linear diffusion equation", 1974.

[15] A. Nusser, A. Dekel, "Filamentary structure from Gaussian fluctuations using the adhesion approximation", *Astrophysical Journal*, Vol. 362, pp. 14-24, Oct. 1990.

[16] D. H. Weinberg, J. E. Gunn, "Largescale Structure and the Adhesion Approximation", *Monthly Notices of the Royal Astronomical Society*, Vol. 247, p. 260, Nov. 1990.

[17] L. Kofman, D. Pogosyan, S. F. Shandarin, A. L. Melott, "Coherent structures in the universe and the adhesion model", *The Astrophysical Journal*, Vol. 393, pp. 437-449, Jul 1992